INTRODUCTION AND REGIONAL GEOLOGY

INTRODUCTION AND REGIONAL GEOLOGY

1.1 INTRODUCTION

Combined, the Proterozoic northern Australian McArthur Basin and Mt Isa Block (Fig. 1.1) form one of the richest base metal provinces in the world. In its own right, the Eastern Succession of the Mt Isa Block (Fig. 1.2), including the Cloncurry District and Mary Kathleen Fold Belt (Fig. 1.3), is also a significant metallogenic district, hosting world-class Ag-Pb-Zn (e.g. Cannington) and Fe-oxide-Cu-Au (e.g. Ernest Henry) deposits. Due to the well exposed nature of rocks throughout much of the region, the Eastern Succession is truly one of the world's best laboratories in which to study the interplay between mineralisation and broader scale structural, metasomatic and other processes. Amongst other research topics, past work in the Eastern Succession has done much in characterizing the nature of Fe-oxide-related Cu-Au mineralisation, and in developing genetic models for these deposits. However, on a global basis, various aspects of this relatively newly recognized class of mineral deposits, including the source of metasomatic fluids and the role of district scale processes in mineralisation, remain contentious. For example, in the Eastern Succession, most researchers appeal to a predominantly magmatic source of saline metasomatic fluids, while in other districts, other fluid sources seem plausible, with intrusive bodies being appealed to only as heat engines driving hydrothermal fluid flow. Further clarification of the contribution of district-scale structural, metamorphic, igneous and metasomatic processes towards mineralisation is critical in developing more robust exploration models for Fe-oxide-Cu-Au mineralisation.

In the Eastern Succession, brecciation is extremely widespread, particularly within Mary Kathleen Group stratigraphy, and is commonly accompanied by intense metasomatism of various affinities. Despite their widespread distribution, Mary Kathleen Group breccias have received little research attention outside the limits of known ore deposits. This oversight has resulted in a gap in our understanding of the geologic evolution of this important region. It is this gap that this thesis aims to fill, with specific reference to the mechanical processes

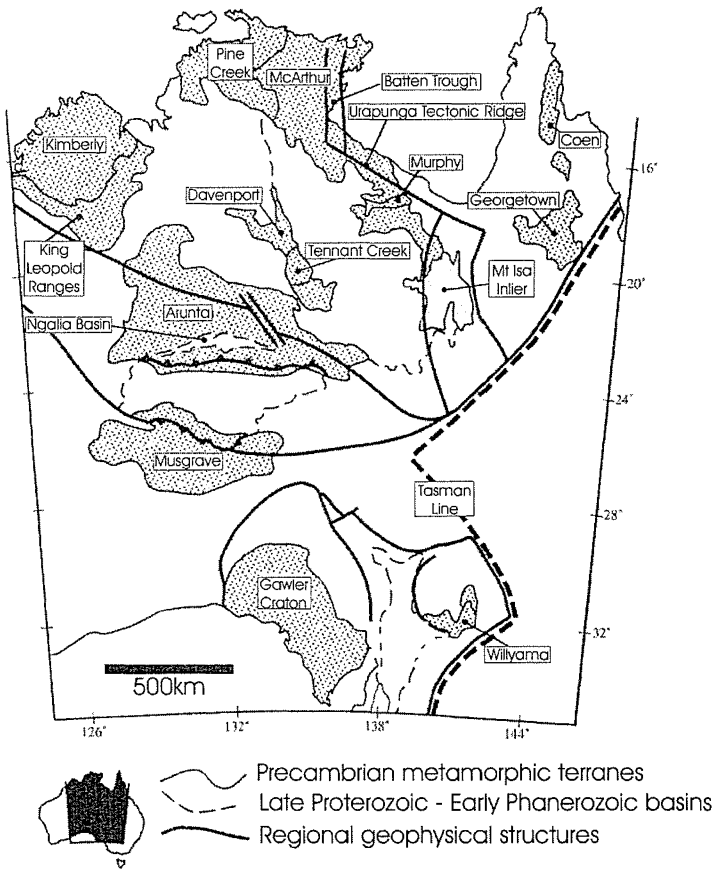

FIGURE 1.1.
Location of the Mt Isa Inlier with respect to other Precambrian terranes within Australia (modified from O'Dea et al., 1997).

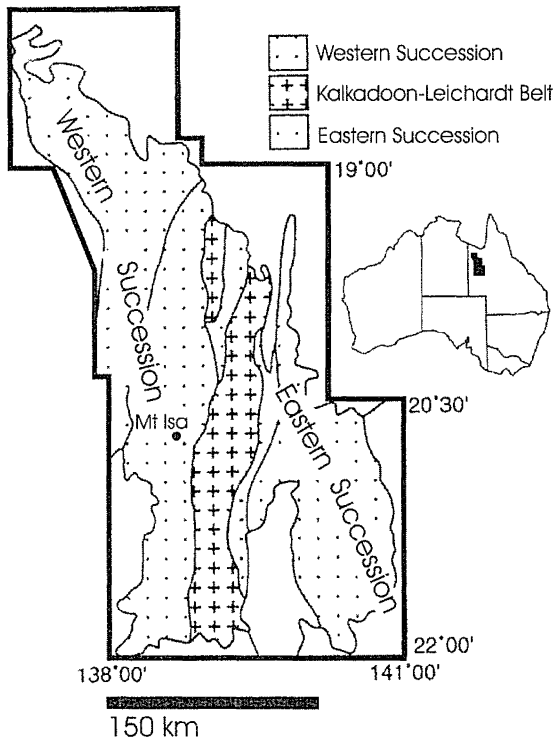

FIGURE 1.2.
Tectonostratigraphic subdivisions of the Mt Isa Block (modified from Blake, 1987).

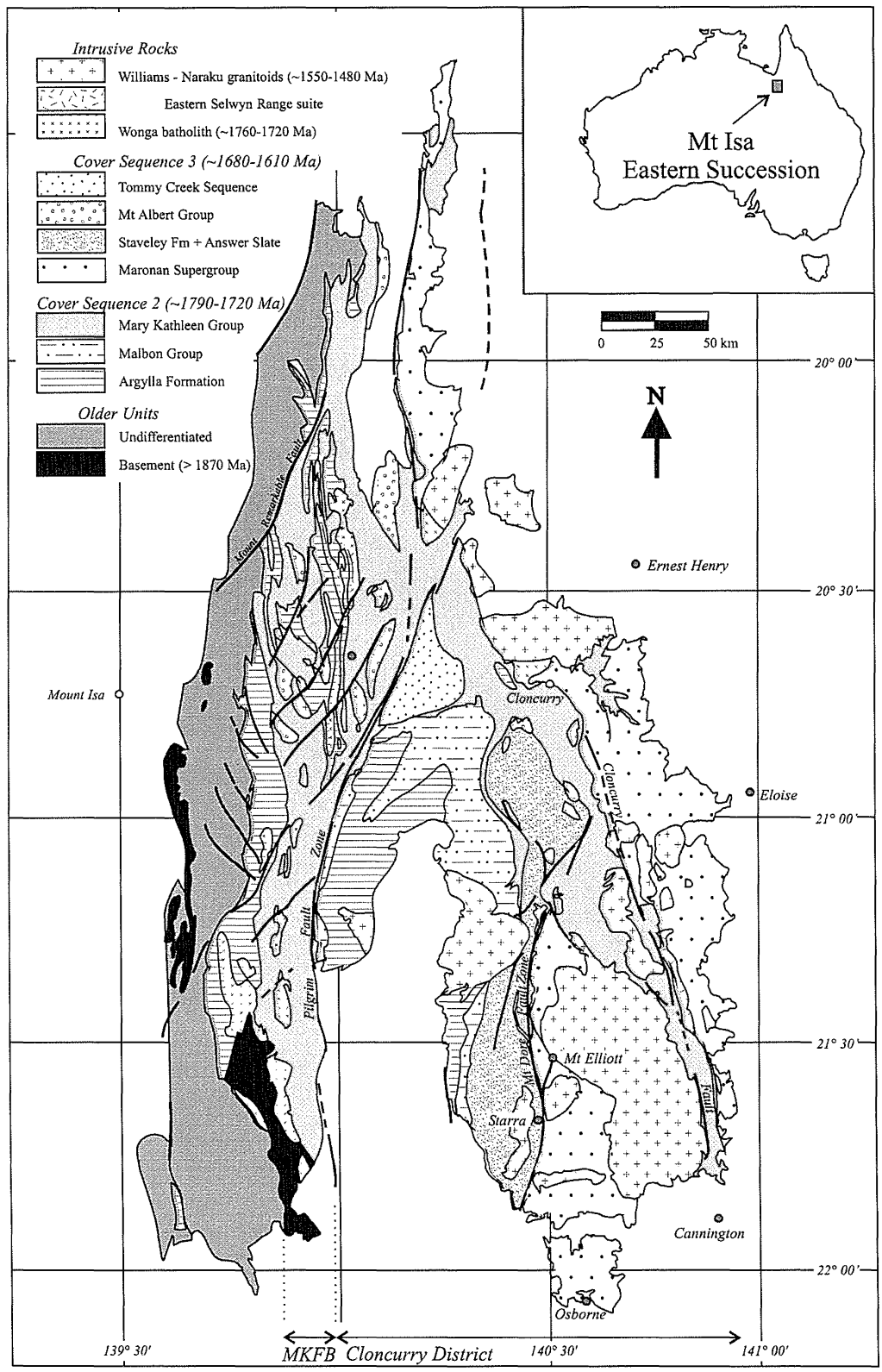

FIGURE 1.3.
Simplified geology of the Eastern Succession, Mt Isa Block (modified from Williams, 1998, and Giles and MacCready, 1997).

associated with brecciation, and the role of brecciation in controlling metasomatic fluid flow. The thesis also addresses the chemical nature of metasomatism associated with brecciation, an appraisal of which is fundamental in understanding how different metasomatic systems relate to one another, and to Fe-oxide-Cu-Au mineralisation. Research presented herein has implications for our understanding of the genesis of Fe-oxide-Cu-Au mineralisation, as well as broader insight into the nature of, and controls on mid-crustal fluid flow.

1.2 THESIS AIMS

While recent research has shed light on many aspects of the geologic history of the Eastern Succession, and the genesis of Fe-oxide-Cu-Au mineralisation in general, there remains much to be learned both about and from this complex terrane. The specific aims of the thesis are as follows:

1. *To produce geological maps at a variety of scales, delineating the distribution of brecciation and metasomatism within portions of the Mary Kathleen Group of the Eastern Succession.*

While previous work has indicated that brecciation and metasomatism are widespread in the Eastern Succession (e.g. Oliver et al., 1993; de Jong and Williams, 1995; Rubenach and Lewthwaite, 2002), little work has been focussed within Mary Kathleen Group stratigraphy of the Cloncurry District. Constraining the distribution of breccias and metasomatic rocks in this area is of key importance in any critical assessment of the genesis of these features, and in clarifying their potential role in mineralisation.

2. *To further constrain the structural history of a portion of the Eastern Succession, with particular reference to brecciation within Mary Kathleen Group stratigraphy.*

Difficulties in correlating structures in brecciated Mary Kathleen Group rocks of the Eastern Succession have proved a hindrance in understanding the structural history of the region. This study aims to place regional brecciation within a comprehensive geologic framework for the Eastern Succession.

3. *To establish the mechanical controls on brecciation in the Eastern Succession and the role of brecciation in controlling metasomatic fluid flow.*

The present study area contains one of the most extensive breccia systems on the planet, and as such provides an ideal environment in which to study the mechanical controls on a variety of different styles of brecciation. As well, the influence of brecciation on the fluid flow regime during widespread metasomatism and more localized Cu-Au mineralisation is addressed.

4. *To characterize the chemical nature of regionally extensive metasomatic systems in the Eastern Succession, and to clarify the role of these systems in the genesis of Fe-oxide-Cu-Au mineralisation.*

While Fe-oxide-Cu-Au deposits are typically associated with regionally extensive alteration systems, the role of these alteration systems in mineralisation remains contentious. The present study aims to clarify the contribution of regional alteration processes to ore systems processes, with specific reference given to the source of metasomatic fluids and the role of fluid-wallrock interaction.

1.3 RESEARCH TOOLS AND METHODOLOGY

1.3.1 Field mapping, core logging and hand specimen observations

This thesis relies in large part on fieldwork undertaken by the author over the course of approximately nine months between 2000 and 2002. Geological mapping, including structural and alteration mapping were undertaken at scales between 1:100 and 1:25000, using tape and compass grids, and airphotos as map bases. Field mapping and observations were supplemented by interpretation of

detailed aeromagnetic data courtesy of Mount Isa Mines Exploration. Approximately 1000 hand specimens were cut and examined to supplement field observations, and approximately half of these were given rankings as to the intensity of various brecciation and alteration parameters for use in the preparation of brecciation and alteration distribution maps. Drill core logging of breccia characteristics was also undertaken at the Ernest Henry deposit.

1.3.2 Structural interpretation

Interpretation of structural data is based predominantly on standard techniques including the use of stereonets, orthographic projection and calculations of fluid pressure gradients. In **Chapter 2**, interpretations of the 3D geometry of structures in the Eastern Succession also draws on wavelet processed aeromagnetic data made available by Mount Isa Mines Exploration.

1.3.3 Analytical samples

Analytical samples were collected during the course of field mapping and core logging. Additional samples from Ernest Henry, and from the Mt Elliott and Eloise deposits are from James Cook University (JCU) thesis collections, and courtesy of other researchers in the School of Earth Sciences, JCU. Characterization of metasomatic assemblages is based on field and hand sample observations, and on petrographic observations from over 200 thin sections.

1.3.4 Mineral chemistry

Major element chemical analyses of silicate and carbonate minerals, and trace element analyses of oxide minerals were undertaken in order to characterize metasomatic mineral assemblages, and to track variations in different chemical parameters. Major element chemistry (silicates, carbonates) was determined using standard microprobe techniques, and is compared with data compiled from a number of previous studies. Trace element compositions of oxides were investigated using laser ablation inductively-coupled-plasma mass spectrometry (LA-ICPMS).

1.3.5 Isotopes

The $\delta^{18}O$ signature of silicates and oxides and the $\delta^{18}O$, $\delta^{13}C$ and $^{87}Sr/^{86}Sr$ signatures of carbonate minerals were analyzed in order to identify fluid sources and temperatures of different metasomatic associations, as well as to assess the role of wallrock interaction on fluid chemistry. This data is compared with similar data compiled from a large number of previous studies.

1.4 THESIS STRUCTURE

This thesis is presented as eight chapters, as outlined below. **Chapters 2** through **7** are intended as stand-alone manuscripts, written in the style of journal articles, and as a consequence there is some repetition of background information between the chapters. Figures are interleaved with the text throughout, and tables are presented following each chapter. A single reference list is given following the final chapter. Analytical data is available in attached appendices, and as EXCEL spreadsheets on an accompanying CD-ROM.

Chapter 1. Introduction and regional geology

Chapter 2. Complexities in the regional structural geometry of the Eastern Succession, Mt Isa Block, Australia

Chapter 2 investigates the structural geology of selected areas within the Eastern Succession. The principal aim of the chapter is to place structural features within a coherent framework, so as to provide a basis for interpretations in subsequent chapters. Documented structural features are consistent with having formed in a west-vergent fold and thrust belt developed during the Isan Orogeny as proposed by O'Dea et al. (1997). Variations in fold patterns away from average north-south trends reflect strain accommodation by reactivation of early faults, stress reorientation around competent intrusive bodies, and forceful displacement of wallrocks during plutonism.

Chapter 3. Volume gain folding and effective layer thinning as modifications on models of tangential longitudinal strain

In **Chapter 3**, variations on the tangential longitudinal strain model for buckle folding are presented. The model variations can be used to explain fold-related fractures that transect competent layers. The proposed variations, 'volume gain folding' and 'effective layer thinning' are described independently from descriptions of Eastern Succession breccias, as in many cases the high strain and complex deformation history of these rocks precluded unambiguous interpretation of fracture timing and mechanism. Nonetheless, the proposed model variations may prove useful in relating fracture geometries to folds in less complex terranes.

Chapter 4. Control of buckle folding and the local stress field on the distribution of widespread magmatic-hydrothermal brecciation in the Cloncurry District, Mt Isa Block, Australia

Chapter 4 outlines the mechanical controls on widespread, late tectonic brecciation in the Cloncurry District. Retrograde folding was accompanied by fracturing, as well as being imposed on rocks that were fractured and boudinaged during prior events. Resultant features include chaotic folded boudin trains and both stratabound and discordant breccia bodies. While brecciation was facilitated to a large degree by fluid overpressuring and high strain rates associated with pluton emplacement, local stress fields active during buckle folding in part controlled the geometry of breccia bodies. Further, brecciation resulted in a net decrease in the competence of some rock units, reducing resistance to flow mechanisms, and allowing for the accommodation of some buckle-fold related space problems. Widespread breccias allowed metasomatic fluids access to large volumes of rock from which some ore components may have been sourced.

Chapter 5. Dynamics of dilational fault zone brecciation and veining in mesothermal ore environments with examples from the Mt Isa Block, Australia

Narrowing in from the focus of the previous chapter, **Chapter 5** addresses the mechanics of dilational fault zone brecciation and veining processes. Specifically, critical parameters including fault mode, the geometry and length of dilational fault segments and wallrock permeability are addressed using examples from barren and mineralized systems in the Eastern Succession. Variations in these parameters during dilational fault slip produced a variety of structures including large width veins, attrition breccias, magmatic-hydrothermal breccias and implosion breccias, as well as fluidized and gas stream breccias. The role of these features in focussing metasomatic fluid flow and the relevance of this focussing to mineralisation processes is also addressed.

Chapter 6. Silicate and oxide mineral and isotope geochemistry as monitors of fluid chemistry in district-scale metasomatic processes, Eastern Succession, Mt Isa Block

In **Chapter 6**, the nature and distribution of regional alteration is documented using petrographic observations and alteration distribution maps. Mineral chemistry and stable isotope data from these assemblages is compared with analyses from igneous and igneous-hosted metasomatic assemblages, and ore-proximal metasomatism. Predictable variations in isotopic ratios and various chemical parameters indicate shifts from igneous-hosted through to metasedimentary-hosted and ore-proximal assemblages. The data is consistent with metasomatic fluids being derived from, or thoroughly equilibrated with igneous rocks, and indicates that variations in ore proximal alteration assemblages reflect varying degrees of cooling and/or wallrock interaction en route to mineralisation sites.

Chapter 7. Fluid sources and fluid-wallrock interaction in regional alteration and iron oxide-Cu-Au mineralisation, Eastern Succession, Mt Isa Block: Insight from C, O and Sr isotopes

Chapter 7 addresses similar questions to those investigated in **Chapter 6**, but using stable ($\delta^{13}C$ and $\delta^{18}O$) and radiogenic ($^{87}Sr/^{86}Sr$) isotopes, cathodoluminescence imagery and mineral chemistry, all from carbonate minerals. This approach has allowed for an unambiguous recognition of magmatic fluid sources, as opposed to fluids of other sources having equilibrated with magmatic rocks. Magmatic fluids are implicated in both regional Na-(Ca) alteration, and Cu-Au mineralisation. Meteoric fluids are evident in paragenetically late, low temperature alteration assemblages, but these do not appear to have played a significant role in mineralisation. The data also highlights the effects of fluid-wallrock equilibration, and confirms the concepts presented in **Chapter 6** that variations in ore-proximal metasomatic assemblages reflect varying degrees of fluid-wallrock equilibration.

Chapter 8. Synthesis and Conclusions

The principal findings of this thesis are summarized in **Chapter 8** and integrated with existing genetic models for Eastern Succession Fe-oxide-Cu-Au mineralisation. Suggestions for future research directions are also proposed.

1.5 PREVIOUS RESEARCH

The northern Australian Mount Isa Block (Fig. 1.1) is a complex Proterozoic terrane that has experienced a protracted tectonothermal history. Key aspects of this history, as documented by previous workers, are summarized in the following section, with emphasis on brecciation and metasomatism in the Eastern Succession.

1.5.1 Tectonostratigraphic zones within the Mt Isa Block

The Mt Isa Block has been subdivided into three approximately N-S trending structural and sedimentological domains (Blake, 1987). These are, from west to east, the Western Succession, the Kalkadoon-Leichardt Belt and the Eastern

Succession (Fig. 1.2). Sedimentary sequences of the Mt Isa Block comprise two major tectonostratigraphic cycles, both of which are interpreted to have been deposited in intraplate sedimentary basins (Blake, 1987). The older of the two sequences predates the Barramundi Orogeny (1900 - 1870 Ma) during which it was metamorphosed and deformed (Blake, 1987). These rocks now comprise the basement to the Mt Isa Block, occurrences of which crop out in the Western Succession. Younger volcanic and sedimentary rocks dominate exposures in the Mt Isa Block, and have been divided by Blake (1987) into three cover sequences, thought to represent at least four episodes of intracratonic rifting (Blake, 1987; Blake and Stewart, 1992; O'Dea et al., 1997). Cover Sequence 1 (1870 - 1850 Ma), exposed in the Kalkadoon-Leichardt Belt, consists of felsic volcanics and comagmatic granites and is thought to have marked a basement high separating two basins now exposed in the Western and Eastern Successions. Cover Sequence 2 (~1790 - 1720 Ma) is dominated by bimodal volcanics and clastic and carbonate metasediments, while Cover Sequence 3 (~1680 - 1610 Ma) comprises rhyolites, dolerites, sandstones and mudstones. Deposition of Cover Sequence 3 ceased with onset of the Isan Orogeny at ~1600 Ma.

1.5.2 Tectonostratigraphic sequences of the Eastern Succession

The Eastern Succession of the Mt Isa Inlier, in which research for this thesis has been carried out, can be further divided into the Mary Kathleen Fold Belt (MKFB) and the Cloncurry District, the two regions being separated by the Pilgrim fault zone (Fig. 1.3). Rocks of Cover Sequences 2 and 3 crop out in the Eastern Succession. Geochronological ages for the Eastern Succession are summarized in Figure 1.4.

Cover Sequence 2

The Magna Lynn metabasalt and clastic sediments and felsic metavolcanics of the Argylla Formation (1783 ± 5 Ma; Page, 1983a) are the lowest stratigraphic units to crop out in the Eastern Succession (Fig. 1.5). Flood basalts (Marraba Volcanics) and clastic sediments (Mitakoodi Quartzite) of the Malbon Group

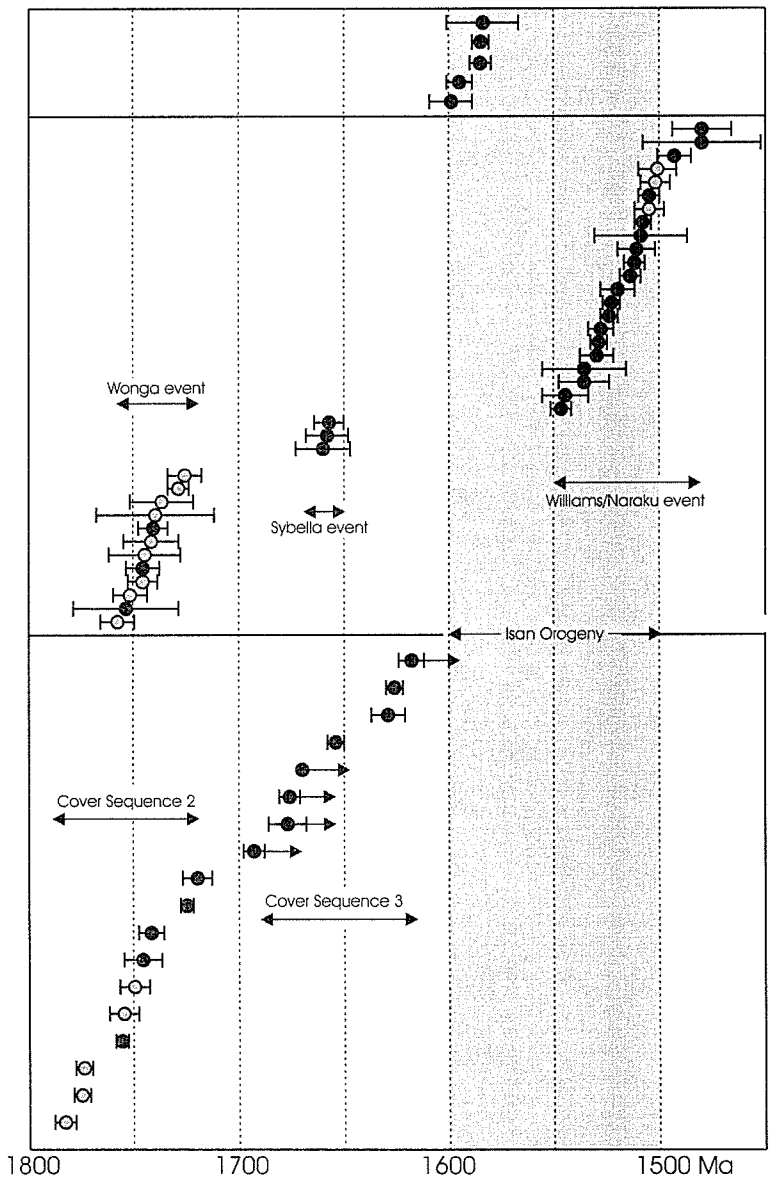

FIGURE 1.4.
Summary of U-Pb geochronological ages from the Eastern Succession including metamorphic ages (top), intrusive crystallisation ages (middle) and sedimentary and volcanic depositional ages (bottom). Black and gray symbols are from the Cloncurry District and MKFB respectively. Symbols with arrows indicate maximum depositional ages. Geochronological data is from Davis et al. (2001), Gauthier et al. (2001), Giles and Nutman (2002), Page (1983a and b, 1998), Page and Sun (1998), Page et al. (1997), Pearson et al. (1992), Pollard and McNaughton (1997), Wyborn and Page (1983) and Wyborn et al. (1988).

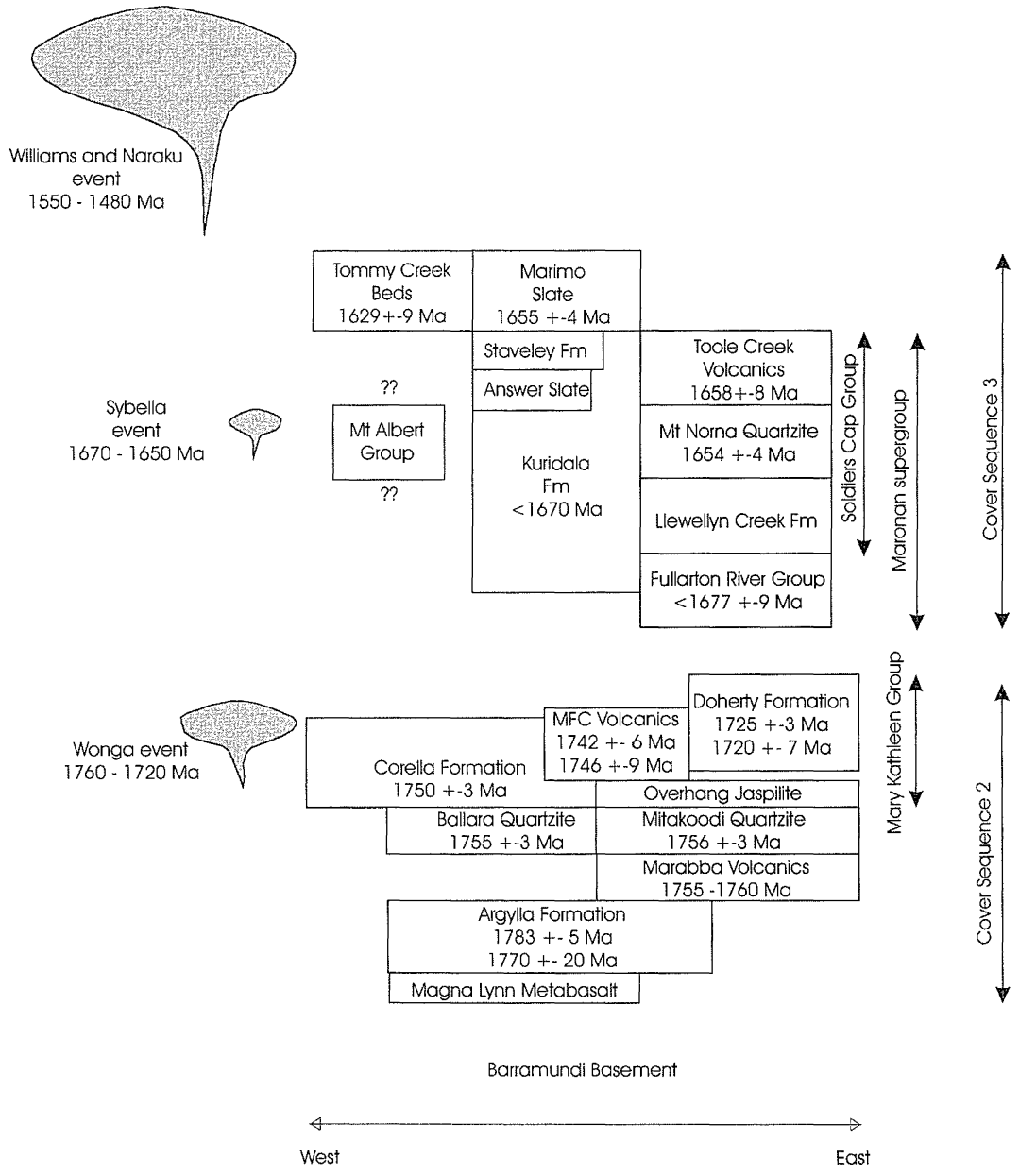

FIGURE 1.5.
Schematic stratigraphic column for the Eastern Succession (modified after Betts et al., 2000). Geochronological data summarized from Davis et al. (2001), Page (1983a and b, 1998), Page and Sun (1998), Page et al. (1988, 1997), Pearson et al. (1992), Pollard and McNaughton (1997), Wyborn and Page (1983) and Wyborn et al. (1988).

overlie the Argylla Formation in the Cloncurry District. In the Mary Kathleen Fold Belt, the Malbon Group is not present, but the Ballara Quartzite appears to be the stratigraphic equivalent to the Mitakoodi Quartzite. Conformably overlying the Ballara and Mitakoodi quartzites, the Mary Kathleen Group includes the calc-silicate rock and marble dominated Corella (1750 ± 7 Ma; Page and Sun, 1998) and broadly equivalent Doherty Formations (1720 ± 7; Page, 1983a; 1725±3 Ma; Page and Sun, 1998). In the northern Cloncurry District, the Mt Fort Constantine felsic volcanics (1746 ± 9 and 1742 ± 6 Ma; Page and Sun, 1998) represent uppermost Mary Kathleen Group stratigraphy.

Cover Sequence 3

The informally named Maronan Supergroup (Beardsmore et al., 1988) contains the Fullarton River Group and the Soldiers Cap Group. The Fullarton River Group, from oldest to youngest, comprises the Gandry Dam Gneiss, Glen Idol Schist and New Hope Arkose, with a combined stratigraphic thickness on the order of 5 km (Beardsmore et al., 1988). Conformably overlying the Fullarton River Group, the Llewellyn Creek Formation, forming the basal unit of the Soldiers Cap Group, is a thick sequence of bedded turbidites. Conformably overlying the Llewellyn Creek Formation, the Mount Norna Quartzite (1654 ±4 Ma; Page and Sun, 1998) contains cross-bedded sandstones, siltstones, mudstones and mafic meta-volcanics. The Toole Creek Volcanics, consisting largely of metabasites and meta-dolerites with minor sediments, conformably overly the Mt Norna Quartzite. Beardsmore et al. (1988) demonstrated that metagreywacke, schist, carbonaceous phyllite, chert and calc-silicate rocks of the Kuridala Formation are stratigraphically equivalent to the Soldiers Cap Group. Sandstones, siltstones and phyllites of the Staveley Formation locally conformably overly the Kuridala Formation (Blake, 1987).

The correlation of the Maronan Supergroup with Cover Sequence 3 elsewhere in the Mt Isa Block has recently come into question. While the Maronan Supergroup shares similar depositional ages with Cover Sequence 3 rocks in the Western Succession, Laing (1998) argued that the two sequences are characterized

by different bulk compositions and varying stratigraphic sequence styles. Furthermore, contacts between the Maronan Supergroup and Cover Sequence 2 rocks are everywhere tectonic, consistent with the hypothesis that the Maronan Supergroup may be an allochthonous terrane (see below and **Chapter 2**). Alternatively, Corella-aged zircons in the Soldiers Cap Group may reflect a proximal basin for deposition of the Soldiers Cap sequences.

The stratigraphic position of the Mt Albert Group, including the feldspathic quartzite dominated Roxmere Quartzite and Lady Clayre Dolomite, remains uncertain, but has tentatively been correlated with Cover Sequence 3 (Blake, 1987).

1.5.3 Structural history

The Mt Isa Block records a complex and protracted structural and metamorphic history. Subsequent to the Barramundi Orogeny, the Mt Isa Block was subject to at least four main deformation events. Wonga-aged extension (ca. 1760-1720 Ma) was followed by the D_1, D_2 and D_3 of the Isan Orogeny, as classified by Bell (1983), and originally proposed for the Western Succession. Several authors have warned about the potential difficulties in extrapolating deformation schemes across complexly deformed terranes. For example, Holcombe and Stewart (1992) cautioned that "a crustal-scale deformation event may be represented by one fabric in one area, but by multiple fabric generations in another, controlled perhaps by the presence or absence of local heterogeneities (...); to go directly to an orogeny-based nomenclature to annotate local structures is scientifically dangerous." More recently, Betts et al. (2000) warned researchers "not to rely on holistic regional correlation of deformation events. In fold and thrust belts individual thrust slices within the system can vary in structural and metamorphic histories, and therefore may not be correlatable." Nonetheless, the D_1-D_2-D_3 framework remains useful in the Eastern Succession and is maintained here, with the recognition that the individual events vary in style within the region, and do not correlate well with events in the Western Succession.

The earliest formed tectonic features recognized in the Eastern Succession relate to a period of sub-horizontal extensional shearing (D_{WONGA}) documented in

the Wonga Belt within the MKFB (e.g. Holcombe et al., 1991; Pearson et al., 1992). This event has not been explicitly recognized elsewhere in the Eastern Succession.

Subsequent to the Wonga event, multiple early thrusting and/or folding events have been appealed to throughout the Eastern Succession (e.g. O'Dea et al., 1997; Lewthwaite, 2000). However, it remains difficult to correlate these events across the Eastern Succession, and while some may be the product of the ~1600-1500 Ma Isan Orogeny, others may be the product of an earlier discrete orogenic event (e.g. Diamantina Orogeny; Laing, 1998). Nonetheless, D_1 is generally accepted as recording emplacement of Cover Sequence 3 rocks over Cover Sequence 2, either by normal faulting, or reactivation of normal faults as thrust faults (see **Chapter 2**).

Tight to isoclinal, N-S trending upright folds and associated axial planar cleavage, commonly synchronous with the peak of metamorphism, dominate outcrop patterns through much of the Eastern Succession. These features appear to be related to a major episode of East-West directed shortening, most commonly attributed to D_2. In addition to well-developed folding, a number of major shear and fault zones in the Eastern Succession have been attributed, at least in part, to D_2. These include portions of the Mt Dore, Maronan, Levuka and Eloise shear zones, and the Cloncurry, Pegmont and Pilgrim Fault zones (e.g. Laing, 1998), although many of these record protracted deformation histories.

D_2 structures are overprinted by a variety of features commonly assigned to D_3. In some areas, such as the MKFB, D_2 and D_3 shortening directions were similar, and D_3 strain was in large part accommodated through reactivation of D_2 structures, and/or the development of conjugate NE- and NW-trending D_3 open folds. Holcombe et al. (1992) proposed that D_3 deformation in the MKFB reflected the waning stages of the D_2 compressional event. D_3 in the Cloncurry District is also marked by the development of open folds with NE to NW orientations. In some regions in the Cloncurry District, the distinction between D_2 and D_3 is more pronounced, as many D_2 axial traces either formed in orientations other than N-S, or were rotated away from N-S prior to the onset of D_3.

Post-D_2 strain was also increasingly accommodated through movement on pre-existing and newly developed shear and fault zones. Many of these structures were active during the main intrusive and metasomatic events that affected the Eastern Succession and consequently played a key role in focussing metasomatic fluids. Laing (1998) divided D_3 faults into four classes based on their orientation and apparent offset (F_N: reverse, F_{NW}: dextral, F_{NE}: sinistral, F_W: extensional), and concluded that the displacement on D_3 faults of different orientations is consistent with east-west directed D_3 shortening.

Post-D_3 deformation was predominantly localized within fault zones, and does not appear to have had a significant impact on the presently observed geometry of the district. Laing (1998) argued that given the kinematic coherence of D_3 faults, any subsequent deformation that reactivated this fault array must have also had a dominant component of east-west directed shortening.

Other researchers have recognized additional deformation episodes within restricted portions of the Eastern Succession. These have proven difficult to correlate on a regional basis, and as cautioned above may represent features that are only manifest locally. These include locally developed, shallowly dipping foliations that postdate D_2 folds and predate D_3 structures. These features have been attributed to a $D_{2.5}$ event (Bell and Hickey, 1998), but their influence on the regional geometry of the Eastern Succession remains contentious (e.g. Lewthwaite, 2000). Numerous other locally developed microscopic foliations have been recognized by other workers (e.g. Lewthwaite, 2000; Mares, 1998), but these do not appear to have had a significant impact on the broad-scale structural evolution of the Eastern Succession.

Tectonic framework

The acquisition of seismic data from an E-W transect across the Mt. Isa Inlier has enabled the structural observations outlined above to be placed in a 3D tectonic framework (e.g. Goleby et al., 1996; MacCready et al., 1998; Drummond et al., 1998). Based in large part on this framework, recent studies (e.g. O'Dea et al., 1997; Betts et al., 2000) have interpreted features developed during the Isan

Orogeny in terms of a west-vergent fold and thrust belt (Fig. 1.6). In these studies, significant shortening across extensional faults reactivated as thrust faults (e.g. Overhang Shear; O'Dea et al., 1997), with hangingwall rocks recording nappe-style deformation features, are attributed to D_1 contraction. This deformation is inferred to have thrust younger Cover Sequence 3 rocks of the Tommy Creek Block, Marimo-Staveley Block, and parts of the Maronan Supergroup and Mt Albert Group, westward over older Cover Sequence 2 rocks (O'Dea et al., 1997; Giles and MacCready, 1997; Betts et al., 2000). Continued thrusting gave way to the development of N-S trending, steeply dipping upright folds (D_2, D_3), marking a transition from thin- to thick-skinned deformation.

1.5.4 Metamorphic history

The Mt Isa Block is characterized by high temperature, low pressure metamorphism, with peak metamorphic conditions in higher grade zones estimated at 400-500 MPa and 650° to 700°C (Foster and Rubenach, 2001). Most of the region is characterized by greenschist to upper amphibolite facies rocks, although lower greenschist assemblages are preserved locally. Porphyroblasts commonly record multiple growth episodes, reflecting a complicated history and multiple thermal events.

Corella Formation marbles and calc-silicate rocks in the vicinity of Cloncurry are dominated by biotite zone assemblages correlated with upper greenschist metamorphic conditions. Peak metamorphic temperatures in this area were ca. 550°C (Hingst, 2002; Foster, pers. comm, 2003). In contrast, in the Mary Kathleen Fold Belt peak metamorphic temperatures locally reached ca. 650°C at 300 to 400 MPa (Reinhardt, 1992).

1.5.5 Absolute timing of deformation and metamorphism

Our understanding of the tectono-metamorphic evolution of the Eastern Succession has improved greatly over the past decade, due in large part to improved geochronological constraints. In the MKFB, Pearson et al. (1992) placed extensional deformation of the Wonga event between ~1760 and 1720 Ma. A

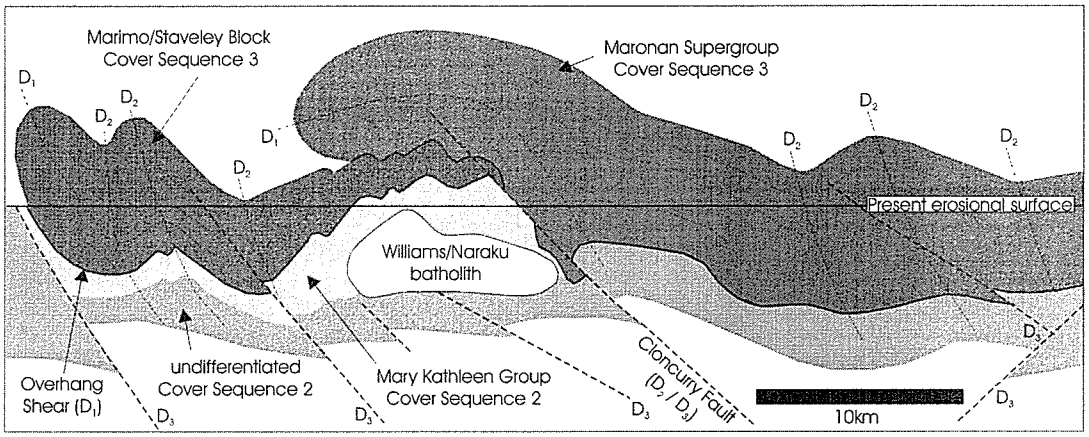

FIGURE 1.6.
Schematic E-W cross-section interpreting the Eastern Succession in terms of a west-vergent fold and thrust belt (modified from Giles and MacCready, 1997).

maximum age of ca. 1610 Ma for D_1 emplacement of Cover Sequence 3 over Cover Sequence 2 can be inferred from depositional ages for the Mt Norna Quartzite (1654 ± 4 Ma; Page and Sun, 1998), the Marimo Slate (ca. 1655 to 1610 Ma; Page et al., 1997), and the Tommy Creek beds (1626 ± 4 Ma; Page and Sun, 1998).

D_2 has previously been interpreted as having occurred at ca. 1550-1540 Ma, based in part on a U-Pb uraninite age of ca. 1550 Ma from the Mary Kathleen U-REE deposit (Page, 1983b). However, given that the deposit is localized by the Mary Kathleen shear zone which cuts D_2 syn-peak metamorphic folds, the 1550 Ma age must be considered a minimum age for D_2 and associated peak metamorphism in that area. Similarly, Page and Sun (1998) report U-Pb igneous zircon ages from the Boorama Tank gneiss and the Marramungee granite of 1547 ± 5 and 1545 ± 11 Ma respectively. While these foliated intrusions have been considered by some authors to be emplaced pre- to syn-D_2, work by Newbery (1990) and de Jong (1995) suggests that they were emplaced into post-D_2 shear zones, and as such may also provide minimum ages for D_2.

More recent evidence for the timing of peak metamorphism in the Eastern Succession include:

1) a 1584 ± 17 Ma U-Pb age from metamorphic zircon rims from the Gandry Dam gneiss north of the Cannington deposit (Page and Sun, 1998),
2) Re-Os ages of 1595 ± 5 and 1600 ± 6 Ma for molybdenite from the syn-metamorphic Osborne deposit (Gauthier et al., 2001),
3) a U-Pb titanite age of 1595 ± 6 Ma (Gauthier et al., 2001), also from the Osborne deposit,
4) U-Pb monazite ages of 1585 ± 4 Ma and 1585 ± 5 from the host rocks to the Cannington deposit and 1599 ± 10 Ma from metamorphic monazite in the Middle Creek Anticline (Giles and Nutman, 2002),
5) ca. 1570 Ma U-Pb monazite ages from the Rosebud Syncline in the MKFB (Hand and Rubatto, 2002), and
6) Sm/Nd garnet ages of ca. 1585 and 1575 Ma from the Tommy Creek Block (Hand and Rubatto, 2002).

Thus, it is now increasingly evident that peak metamorphism occurred at ca. 1600-1570 Ma throughout much of the Eastern Succession. Given the common assertion that D_2 isoclinal folds and associated cleavages formed broadly synchronous with peak metamorphism, an approximate age of 1600-1570 Ma seems most likely for D_2 deformation in the Eastern Succession (N.B. D2 and peak metamorphism in the Western succession appear to be some 50 million years younger).

In the MKFB, D_3 is constrained by a U-Pb titanite age of 1530 - 1525 Ma (Oliver et al, submitted). Mark and de Jong (1996) placed the age of D_3 in the Cloncurry District at ~1527, based on dates of foliated (1529 ± 4 Ma) and unfoliated (1523 ± 4 Ma) granitoids of the Mt. Angelay intrusive complex. This range of ages suggests that the D_3 event spanned the interval from approximately 1530 to 1520 Ma.

Thermochronological data presented by Spikings et al. (2001) suggests that currently exposed Eastern Succession rocks cooled to temperatures of ~220°C between ~1500 and 1400 Ma. Subsequent thermal events episodically raised regional temperatures no higher than 250° to 275°C (Spikings et al., 2001). Locally however, higher temperatures may have been reached, such as in the vicinity of the Lakeview Dolerite (1116 ± 12 Ma; Page, 1983b).

1.5.6 Intrusive events

Wonga event

Prior to deposition of Cover Sequence 3, intrusions of the Wonga batholith were emplaced in the Mary Kathleen Fold Belt between ca. 1760 and 1720 Ma. Intrusion was coincident with, and facilitated by the Wonga extensional event (Holcombe et al., 1992; Pearson et al., 1992) and was accompanied by extensive NaCl-rich scapolitization, skarn development and Na-(Ca)-K metasomatism. The evaporitic Corella Formation has been considered as a likely source of salt during this metasomatic event (Ramsay and Davidson, 1970; Oliver et al., 1994).

Intrusions of similar age also occur in the Cloncurry District and include the Gin Creek and Jessie granites (1741 ± 7 and 1746 ± 8 respectively; Page and Sun,

1998). Based on their location, these have been classified as phases of the Williams and Naraku batholiths, while their ages indicate that they represent an easterly extension of the Wonga intrusive event (e.g. Davis et al., 2001).

Sybella event

The Ernest Henry Diorite (1660 ± 13, 1658 ± 10, 1657 ± 7 Ma; Pollard and McNaughton, 1997) of the Cloncurry District was emplaced synchronously with the Sybella Granite (1660 ± 4 Ma, 1655 ± 5 Ma; Connors and Page, 1995) in the Western Succession of the Mt Isa Block at ~1660 - 1655 Ma. However, the Ernest Henry Diorite, found only in drill core west of the Ernest Henry Cu-Au deposit, is geochemically more primitive than its Western Succession counterpart, and it remains unclear if these intrusions are genetically related.

Williams and Naraku event

The Williams and Naraku batholiths contain multiple intrusive phases emplaced during the Wonga event (~1750-1730 Ma), the Sybella event (~1660 Ma) and dominantly during the Williams and Naraku event (~1550-1480; Page and Sun, 1998), including plutons of the Eastern Selwyn Range Early Granite Suite (~1545 Ma; Fig. 1.3). The most volumetrically abundant of the intrusions that make up the Williams and Naraku batholiths are typically K-rich granites, emplacement of which was coincident with major phases of Na-(Ca) alteration and Fe-oxide-Cu-(Au) mineralisation in the Cloncurry District.

Pollard et al. (1998) subdivided the 1550 Ma and younger intrusion of the Cloncurry District into the Cloncurry and Eureka Supersuites, based on mapping and whole rock geochemistry. The Cloncurry Supersuite contains subalkaline, high-K, metaluminous monzogranite and syenogranite. The Eureka Supersuite contains alkaline, K-rich shoshonites ranging from diorite to syenogranite, and are temporally related to extensive Na-(Ca) alteration in the Cloncurry District.

Volumetrically minor intrusions with similar structural timing to the main Williams and Naraku plutons (post-D_2 and pre- to post-D_3) also occur in the MKFB. Some of these, previously mapped as Burstall Granite, likely represent a westward

extension of the Williams and Naraku intrusive event. Pegmatitic intrusions coincident with the main intrusive phases in the Williams and Naraku batholiths are also present in the Western Succession (1532 ± 7 Ma; Connors and Page, 1995).

1.5.7 Brecciation

A number of studies have focussed solely or in part on the structural evolution of portions of the Eastern Succession (e.g. Oliver et al., 1991; Pearson et al., 1992; Holcombe et al., 1992; Lally, 1997, O'Dea et al., 1997; Betts et al., 2000; Lewthwaite, 2000). Despite this high level of research into the structural evolution of the region, and while many authors have touched on the topic brecciation, relatively few studies have addressed in detail the mechanical controls on brecciation.

Early researchers have considered Mary Kathleen Group breccias as pyroclastic deposits (Honman et al., 1939), transported reef breccias (Carter et al., 1961), intraformational breccias (Derrick, 1969), and fold breccias related to batholith emplacement (Glikson, 1972). However, early work lacked the present level of understanding of the structural evolution of the region, and in several cases contains interpretations that are clearly inconsistent with what is now known about the region's geology and geochronology.

Several more recent studies have touched on brecciation processes but have not provided rigorous interpretations of breccia genesis. For example, Laing (1998) suggested that massive dissolution accompanied diapirical uplift of Corella Formation rocks, yet provided no evidence for this, or constraints on the timing or mechanisms of this event. Given the evaporitic nature of Mary Kathleen Group stratigraphy, salt diapirism certainly seems likely during diagenesis and early stages of metamorphism. However, extensive evidence points to a post-peak metamorphic timing for much of the brecciation in the Mary Kathleen Group.

Ryburn et al. (1988a) suggested that the Gilded Rose Breccias, which they considered as a subset of the Corella Breccias, are hydrothermal intrusive breccias related to late tectonic granitoid emplacement, yet on accompanying geological maps and cross-sections (Ryburn et al., 1988b) these were depicted as thin surficial

veneers. Ryburn et al.'s (1988a and b) distinctions between the Corella breccias and Gilded Rose breccias are maintained for the purposes of discussion in this contribution. However, the distinction between the breccia styles is based in part on inferred genetic mechanisms, as well as diagnostic features that are not necessarily mappable in the field. As such, breccia distribution maps in **Chapter 4** do not correspond with Ryburn et al.'s (1988a and b) subdivisions.

Blake et al. (1982) considered the matrix of the Mount Philp breccias in the Mary Kathleen Fold Belt to have crystallized from a melt, despite providing geochemical analyses which they admitted were inconsistent with the chemistry of any known unaltered igneous rock. Tunks (1987) recognized two classes of breccias within Corella Formation rocks of the Cloncurry District, which he termed 'Early breccias' and 'Late breccias'. Tunks attributed the genesis of the 'Early breccias' to a combination of solution collapse processes in response to dissolution of evaporitic beds, thrusting, and boudinage-related processes in layers of contrasting competence. The 'Late breccias' of Tunks were attributed to retrograde boiling and decompression associated with felsic intrusion. Several mechanisms proposed by Tunks (1987) are given a more rigorous assessment in this study.

Oliver et al. (1990 and 2001a) considered stress reorientation around competent meta-intrusive bodies and early formed skarns to have played a key role in localizing brecciation and associated alteration of Corella Formation rocks in the MKFB. The results from Oliver's research have key implications for this study and will be revisited in more detail in **Chapter 5**.

De Jong and Williams (1995) provided evidence confirming that extensive hydrothermal breccias adjacent to the Cloncurry fault acted as important conduits and hosts for intense Na-(Ca) and later (K)-Fe alteration. Structural features noted by these authors range in character from brittle-ductile shear zones to purely brittle fractures, with brecciation associated with both brittle and ductile features.

A number of other researchers have touched on breccia genesis issues as relevant to specific Fe-oxide-Cu-Au deposits (e.g. Adshead, 1995; Pollard et al.,1997a; Twyerould, 1997; Davis, 1997; Little, 1997; Adshead-Bell, 2000). Some of these interpretations are revisited in **Chapter 5**.

1.5.8 Metasomatism

A number of researchers have investigated the chemical nature of hydrothermal fluids associated with alteration and mineralisation, both within and distal to ore deposits in the Eastern Succession of the Mt Isa Block. Detailed isotope, fluid inclusion, whole rock geochemistry, electron microprobe and more recently Laser-Ablation ICP-MS and proton induced X-ray emission (PIXE) analysis have done much to shed light on the chemical nature and source of hydrothermal fluids involved in various styles of alteration and mineralisation. Williams and Blake (1993), Oliver (1995) and Pollard et al., (1997b and c) provide comprehensive reviews of much of this earlier work, while Mark and Foster (2000), Perring et al. (2000), Williams et al. (2001) and Rubenach and Lewthwaite (2002) amongst others provide more recent investigations.

Magmatic-hydrothermal interface rocks

In the central Cloncurry District, Tolman (1998) and Mark and Foster (2000) have documented ptygmatic aplite and pegmatite intimately associated with albite, actinolite and apatite ± magnetite and titanite assemblages. These rocks are texturally similar to unidirectional solidification textures (USTs) documented in the roof zones of some porphyry stocks (e.g. Shannon et al., 1982). Also, Perring et al. (2000) documented miarolitic and spherulitic, albite-, magnetite- and quartz-rich (± diopside, K-feldspar, biotite, titanite and pyrite) sills at Lightning Creek in the southern Cloncurry District. At each of these locales, complex textures within intrusive rocks have been interpreted to record fluid exsolution during magmatic crystallisation, and the host intrusions have been appealed to as sources for fluids responsible for regional Na-(Ca) alteration (Mark and Foster, 2000; Perring et al., 2000).

Na-(Ca) Alteration

The most extensive style of alteration in the Eastern Succession is marked by albite and actinolite ± diopside, magnetite, titanite and apatite rich mineral

assemblages, and has affected all rock types in the district. Variations in mineralogy are common, and appear to be affected by variations in fluid chemistry, temperature and host rock. Na-(Ca) alteration is commonly associated with brittle-ductile shear zones, brittle fractures and megabreccias, and was caused by high temperature (>400°C) H_2O-CO_2-NaCl fluids (e.g. de Jong and Williams, 1995; Oliver, 1995; Pollard, 2001).

(K)-Fe alteration

More spatially restricted than Na-(Ca) alteration assemblages, (K)-Fe alteration assemblages form the immediate hosts to some Cu-Au deposits in the Eastern Succession (e.g. Starra, Ernest Henry; Rotherham, 1997, Mark and Crookes, 1999). These assemblages vary significantly in mineralogy with variable proportions of K-feldspar, biotite, amphibole, magnetite, hematite, calcite, quartz and chlorite, likely reflecting both fluid composition and temperature. Low temperature (<350°C) K-feldspar ± quartz, hematite, quartz, chlorite and calcite assemblages are also noted, but do not appear to be spatially associated with Cu-Au mineralisation (e.g. de Jong and Williams, 1995).

1.5.9 Mineralisation

The Eastern Succession of the Mt Isa Block is host to significant base and precious metal reserves and a variety of different ore deposit styles. Various authors have presented a number of classification schemes with which to consider the metallogeny of the Eastern Succession (e.g. Williams and Blake, 1993; Davidson, 1998; Laing, 1998). A modified version of the classification of Williams (1998), separating deposits into three classes based on commodity, namely (i) ± Pb ± Zn ± Ag, (ii) (Fe) ± Cu ± Au ± Ag ± Co and (iii) U-REE systems, is summarized below, with additional information from other sources as noted.

±Pb ±Zn ±Ag deposits

Apart from mineralisation at Dugald River, ± Pb ± Zn ± Ag deposits of the Eastern Succession are hosted by amphibolite facies meta-siliciclastic rocks of the

Maronan Supergroup, and are commonly considered as Broken Hill type (BHT) deposits (e.g. Walters and Bailey, 1998). Controversy exists as to whether the deposits, including Cannington, Dugald River, Maronan, Maramungee and Pegmont, are metamorphosed syn-genetic deposits (e.g. Dixon and Davidson, 1996; Bodon, 1998), or metamorphogenic/metasomatic in origin (e.g. Chapman and Williams, 1998; Williams et al., 1998). With respect to Cannington, it is evident that if Ag, Pb and Zn were concentrated at or near the present deposit site synchronously with sedimentation, then this accumulation was not only metamorphosed, but also metasomatised during the Isan Orogeny (e.g. Chapman and Williams, 1998).

(Fe) ± Cu ± Au ± Ag ± Co deposits

Eastern Succession (Fe) ± Cu ± Au ± Ag ± Co deposits, more commonly referred to as Fe-oxide-Cu-Au deposits, are hosted in sulphide ± iron-oxide bodies, with typical ore assemblages of chalcopyrite ± pyrite ± pyrrhotite ± Fe-oxides. Mineralisation is invariably fault or fracture controlled, with most deposits lying within 2 km of major faults (Laing, 1998). Although a broad spatial association is noted with granitic intrusions, mineralisation is generally hosted within metamorphic rocks, commonly within broad zones of Na-(Ca) alteration, and more restricted (K)-Fe alteration.

U-REE deposits

The Mary Kathleen deposit is the only historically mined U-REE deposit in the Eastern Succession. Uraninite and allanite rich ore at the deposit is localised by paragenetically older garnet-pyroxene skarn alteration adjacent to the Mary Kathleen shear zone (Page, 1983b, Oliver et al., 1999).

Relationship between alteration and mineralisation styles

Crystallising intrusive rocks are the preferred source of metasomatic fluids for regional alteration and Cu-(Au) mineralisation in the Eastern Succession (e.g. de Jong and Williams, 1995; Rotherham et al., 1998; Perring et al., 2000). Further, recent models suggest links between regional and ore proximal metasomatism. For

example, Pollard (2001) argued that unmixing of magmatic H_2O-CO_2-NaCl fluids will lead to albitisation of wallrocks at high temperature, giving way to K-feldspar alteration at lower temperatures, due to an increase in the equilibrium Na/(Na + K) in Cl-bearing fluids buffered by alkali feldspars. In a complementary model, Oliver et al. (in revision) proposed that Na-(Ca) alteration results in a progressive increase in the fluid concentrations of KCl and FeCl, until metasomatic fluids become biotite and K-feldspar stable.

Enrichment in U and REEs in some (Fe) ± Cu ± Au ± Ag ± Co deposits may indicate a genetic relationship between some deposits of this class, and the Mary Kathleen U-REE deposit. Some researchers have also proposed magmatic fluid sources for some examples of ±Pb ±Zn ±Ag mineralisation (e.g. Pollard, 1997), potentially indicating a genetic link between these deposits and (Fe) ± Cu ± Au ± Ag ± Co deposits, although this has not been firmly established.

COMPLEXITIES IN THE REGIONAL STRUCTURAL GEOMETRY OF THE EASTERN SUCCESSION, MT ISA BLOCK, AUSTRALIA

COMPLEXITIES IN THE REGIONAL STRUCTURAL GEOMETRY OF THE EASTERN SUCCESSION, MT ISA BLOCK, AUSTRALIA

2.1 INTRODUCTION

In this contribution, the structural history of selected areas within the Eastern Succession of the Mount Isa Block is investigated in order to establish a framework within which the mechanical controls on regional-scale brecciation can be detailed. Structural features in the Eastern Succession are largely attributed to the Mesoproterozoic Isan Orogeny which has recently been interpreted in terms of a west-vergent fold and thrust belt, superimposed on rocks deposited and extruded during a protracted rift history (e.g. O'Dea et al., 1997). Alternatively, some authors have appealed to multiple shifts in compression direction during the Isan Orogeny (e.g. Mares, 1998; Lewthwaite, 2000), but these in turn are difficult to reconcile within a coherent tectonic framework.

Research presented here focuses on the 'Cloncurry Region' (Fig. 2.1), an area characterized by extensive brecciation and regionally anomalous structural patterns. Further observations are drawn from smaller areas within the larger Cloncurry District (Budenberri area) and the Mary Kathleen Fold Belt (Tribulation and Mt Philp areas; Fig. 2.1). The causes of regional variations in structural patterns include effects of superposed folding, reorientation of stress fields around early-tectonic intrusives, reactivation of rift-related fault architecture during compression, and forceful displacement of wallrocks during pluton emplacement. Recognition of the effects of these mechanisms reveals that complex structural patterns can largely be interpreted in the context of prolonged east-west directed shortening.

2.1.1 Previous work

The structural evolution of the Eastern Succession has for some time been thought of in terms of three principle deformation events, D_1, D_2 and D_3, attributed to the Mesoproterozoic Isan Orogeny. This deformation scheme was originally established for the Western Succession of the Inlier (Bell, 1983), and since then has

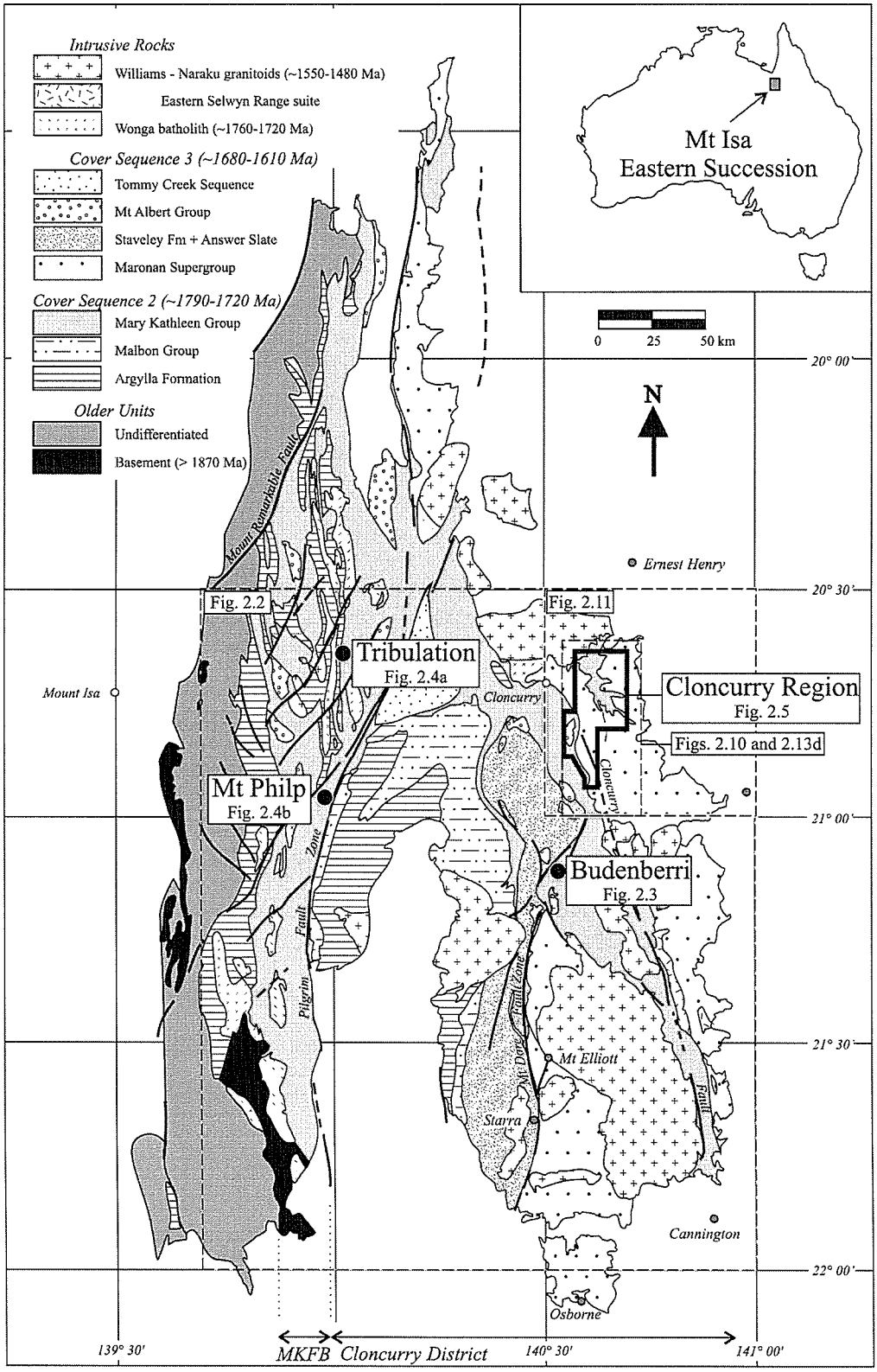

FIGURE 2.1.
Simplified geology of the Eastern Succession, modified after Williams (1998). Locations of study areas addressed in this contribution are indicated.

been somewhat haphazardly extrapolated to the Eastern Succession. Recently, detailed structural investigations (e.g. Lewthwaite, 2000; Betts et al., 2000) and new geochronological data (e.g. Page and Sun, 1998; Giles and Nutman, 2002; Hand and Rubatto, 2002) indicate that structural events do not correlate well between the Eastern and Western Successions. Further, early phases of deformation previously attributed to the Isan Orogeny may be related to the earlier Diamantina Orogeny proposed by Laing (1996) to have affected the Georgetown Inlier, the Willyama Block and the Eastern Succession of the Mt Isa Inlier. With these issues in mind, the deformation history of the Eastern Succession is reviewed, with emphasis on the northern Cloncurry District.

Early rift history

Various authors have outlined a protracted rift history between ca. 1800 and 1600 Ma, during which cover sequences of the Mt Isa Block were deposited or extruded (Carter et al., 1961; Blake, 1987; Etheridge and Wall, 1994; O'Dea et al., 1997). At least four episodes of rifting are evident. Of relevance to this contribution is the deposition of Cover Sequence 2 (Blake, 1987), which commenced at ca. 1790 Ma and was interupted by an episode of sub-horizontal extensional shearing of the Wonga event, with upper block to the north sense of shear (Holcombe et al., 1991). The upper block, comprising predominantly Corella Formation stratigraphy, was characterized by brittle structures, including originally south-dipping listric normal faults. Cover Sequence 3 (Blake, 1987) in the Eastern Succession was largely deposited during the interval between approximately 1680 and 1610 Ma, but basinal geometry remains poorly constrained.

D_1: Thrusting and folding

O'Dea et al. (1997) proposed west-vergent thrusting of younger rocks (Cover Sequence 3) over older rocks (Cover Sequence 2) across the Overhang Shear in the Mitakoodi block and associated isoclinal folding in both the footwall and hangingwall (D_1 of O'Dea et al., 1997; see also Betts et al., 2000). Similarly, Laing (1998) considered the Maronan Supergroup (Cover Sequence 3) to be an

allochthonous terrane, and invoked originally flat-lying mylonitic shear zones to explain the juxtaposition of Cover Sequences 2 and 3 (D_1 of Laing, 1998). In contrast, Lewthwaite (2000) records E-SE striking cleavages and tight to isoclinal folds, from which she inferred an early episode of N-S directed sub-horizontal shortening (G_1 of Lewthwaite, 2000) and synchronous metamorphism. While each of the above structures have been attributed to D_1, conflicting shortening directions likely indicate that "D_1" actually represents multiple deformation events.

D_2: E-W shortening and isoclinal folding

Upright, roughly north-south oriented folds have been assigned to the D_2 event across much of the Eastern Succession. D_2 folds are tight to isoclinal, and exhibit a well-developed axial planar cleavage in all rock units. D_2 folds, including the Snake Creek Anticline (G_2 of Lewthwaite, 2000), are broadly synchronous with upper greenschist to amphibolite facies peak metamorphism, and likely formed at approximately 1600-1570 Ma (Page and Sun, 1998; Giles and Nutman, 2002; Hand and Rubatto, 2002). O'Dea et al. (1997) and MacCready et al. (1998) argued that during D_2 the entire supracrustal sequence (Cover Sequences 2 and 3) was detached from the basement along a major décollement zone, interpreted from the Mt Isa deep seismic transect.

Reorientation of D_2 folds

A number of structural features recognized by various authors throughout the Eastern Succession appear to have developed between the D_2 and D_3 events. These include shallow-dipping cleavages, rare small-scale folds, and the rotation of earlier folds into shallow-dipping orientations evident at a number of localities (Adshead-Bell, 1998; Mares, 1998; Lewthwaite, 2000). Additionally, in the northern Cloncurry District, Lewthwaite (2000) recognized local evidence for N-S directed shortening between D_2 and D_3, which resulted in rotation of the axial trace of the Snake Creek Anticline from N-S to E-W. Similarly, the northern extent of the axial trace of the D_2 Duck Creek Anticline exhibits a rotation from NNE to NNW.

D_3: E-W shortening, heterogeneous folding, reverse and wrench faulting

The D_3 event has been interpreted as marking a transition to thick-skinned deformation producing upright folds, broad flexures in the basement-cover interface, and east-dipping basement cutting faults (O'Dea, 1997, MacCready et al., 1998). D_3 folds are marked by variably NE- to NW-trending axial planes, as noted in studies in the Hampden Synform (Betts et al., 2000), the Snake Creek area (G_4 of Lewthwaite, 2000), and the Mary Kathleen Fold Belt (Holcombe et al., 1992). A well-developed fault array throughout the Eastern Succession was largely active during D_3, and exhibits components of both compressional and wrench tectonics (O'Dea, 1997; Laing, 1998). Absolute timing of D_3 in the Eastern Succession is constrained to approximately 1530-1520 Ma (Mark and de Jong, 1996; Oliver et al., 2001).

2.1.2 Approach and methodology

Interpretations in this study are primarily based on structural mapping, field observations, and conventional stereonet and block diagram interpretations of structural data, as well as interpretation of conventional and wavelet processed aeromagnetic data. Aeromagnetic data is presented in the form of a 2D structural skeleton (Fig. 2.2) produced from total magnetics intensity (TMI) data (courtesy of Mount Isa Mines Exploration). Using the "skeletonize" feature of Scion Image, linear features in the TMI data were reduced to line segments, highlighting structural grains in the region. While the technique does produce some spurious results, most notably straight N-S and E-W oriented line segments in areas of low magnetic intensity, it provides an efficient and objective alternative to manually drawn skeleton maps.

Wavelet processed aeromagnetic data was also used in this study. Wavelet processing (Archibald et al., 1999) is a relatively new technique, which allows for the detection of boundaries separating zones of different density or magnetic susceptibility in potential field data. These edges are projected as series of points that form near-continuous curves or 'worms' at various intervals of constant z-

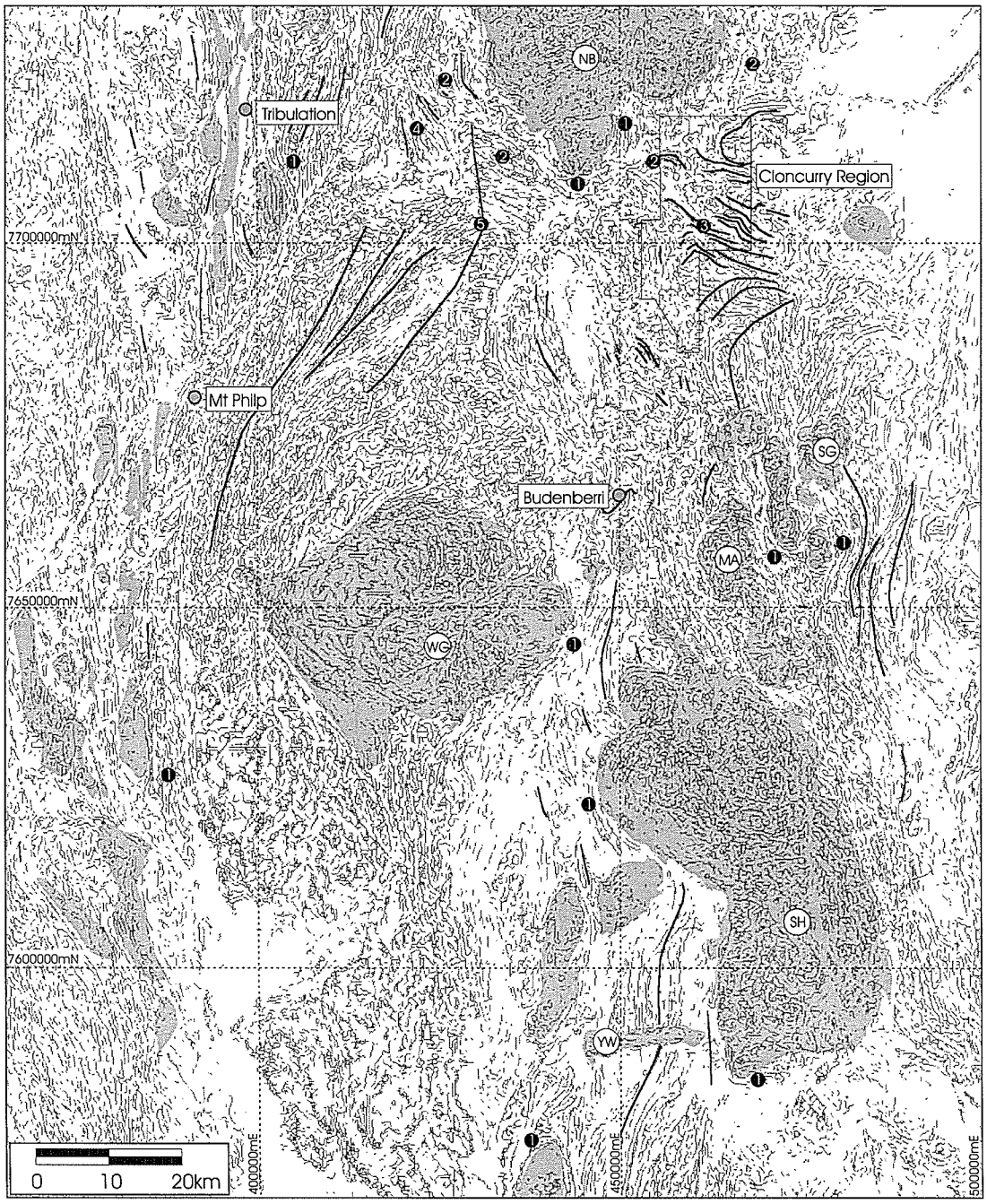

FIGURE 2.2.
Skeleton map of high-resolution TMI aeromagnetic data, covering much of the Eastern Succession. Outcropping extents of major intrusive units are shown in grey. D_2 axial traces are indicated by bold lines. Features of interest include 1) strong anastamosing of structural trends adjacent to some plutons, 2) a broad zone (ca. 5km) of anomalous structural grain around the Naraku Batholith, 3) anomalous structural trends throughout the Cloncurry Region, and 4) NW oriented structures in the northern Tommy Creek Block. WG = Wimberu granite, NB = Naraku Batholith, SG = Saxby granite, MA = Mount Angelay granite, SH = Squirrel Hills granite, YW = Yellow Waterhole granite.

value. Z-values are reported in metres, and reflect the combined influence of the true depth of a given edge in the potential field data, and the coarseness of that edge (Archibald et al., 1999). Thus while wavelet processed data can give an indication as to the dip direction of features, it cannot be used to infer the true dip or true depth of features. Consequently, z-values are typically projected upwards, so as not to give the false impression of reflecting true depth. Further, because continuous coverage exists within, but not between flat lying sections, the process is better for visualizing steeply dipping edges, rather than shallow-dipping features. For this study, 3D form surfaces were constructed from total magnetic intensity (TMI) data, which was wavelet processed by Fractal Graphics. Data was available in the form of points projected at 32 different levels of z-values ranging from 200 to 25 990m.

2.2 STRUCTURAL OBSERVATIONS

2.2.1 Regional structural patterns

While a N-S oriented structural grain is common throughout the Eastern Succession, regional maps and geophysical data reveal significant exceptions, particularly to the east of the Pilgrim Fault (Fig. 2.1). In Figure 2.2, a skeleton map of total magnetic intensity (TMI) aeromagnetic data predominantly reflects primary layering in metasedimentary and metavolcanic units. However, tectonic layering, magnetic fabrics within intrusive units, shears and fault zones are also represented, although the later two are more typically characterized by magnetic lows, and hence linear breaks in the skeleton patterns. Figure 2.2 highlights the complexity of structural patterns throughout the Eastern Succession, and in particular adjacent to some of the major intrusive units in the region. While various authors have addressed the significance of some of the regional variations in structural trends in the Eastern Succession, deviations from the average N-S trend remain difficult to explain in a coherent tectonic model for the whole of the region.

2.2.2 Budenberri area

The Budenberri area lies between the Big Mick and Martin Creek faults in the central Cloncurry District (Fig. 2.1). Two phases of folding are evident in the area (Fig. 2.3). A single early fold crest is tight and exhibits significant hinge-zone thickening. The fold is refolded by an open fold, with a NNE trending, steeply dipping axial plane, and fold axes which plunge moderately to the SSW. Late folding is characterized by negligible hinge-zone thickening, and hinge zone breccia bodies are related to late folding (**Chapter 4**, this study).

2.2.3 Mary Kathleen Fold Belt: Tribulation and Mt Philp areas

Structural mapping was carried out in two regions within the Mary Kathleen Fold Belt. The Tribulation area surrounds the Tribulation and Lime Creek calcite quarries to the north of the abandoned Mary Kathleen U-REE mine (Fig. 2.1). The Mt Philp area lies between the Fountain Ranges and Pilgrim faults (Fig. 2.1), and contains the giant Mt Philp ironstone, and adjacent Mt Philp breccia body.

Mapping in both the Tribulation and Mt Philp areas reveals a consistent N to NNE strike and near vertical dip to axial planar cleavages and fold-limbs (Fig. 2.4), consistent with observations of previous workers in the belt (e.g. Holcombe et al., 1991). Pre-D_2 intrusions of the Burstall and Wonga Suites are elongate parallel to the regional structural trend (N-S) and commonly contain a well-developed foliation parallel to the axial planar cleavage developed in adjacent metamorphic rocks. Elsewhere in the belt, however, Holcombe et al. (1991) and Pearson et al. (1991) mapped km-scale lozenges within the Wonga Granite that preserve evidence for earlier syn-extensional fabrics, although these areas are restricted in extent compared with the dominant N-S grain. While post-D_2 pegmatites are also noted in both regions, these are volumetrically minor, and do not appear to have significantly influenced the structural geometry of their surrounds.

2.2.4 Cloncurry Region

In the following sections, structural features are described within the Cloncurry Region (Fig. 2.1). The deformation scheme is based on overprinting

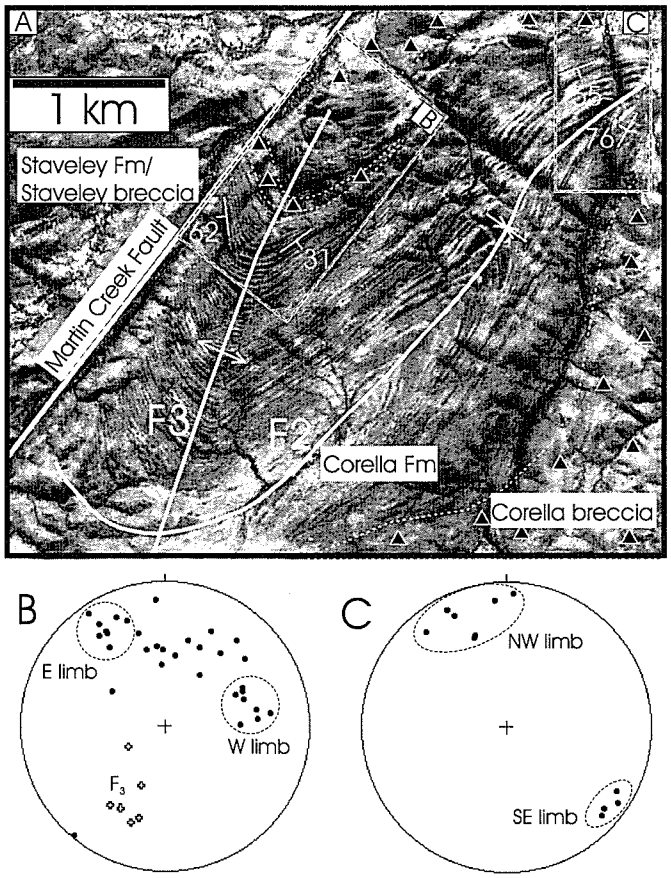

FIGURE 2.3.
(a) Aerial photograph with mapped geology from the Budenberri area. Triangle pattern indicates distribution of brecciation. (b-c) Lower hemisphere, equal area stereonets for data from areas indicated in Figure 2.3a indicate tight and open folds for early and late fold events respectively.

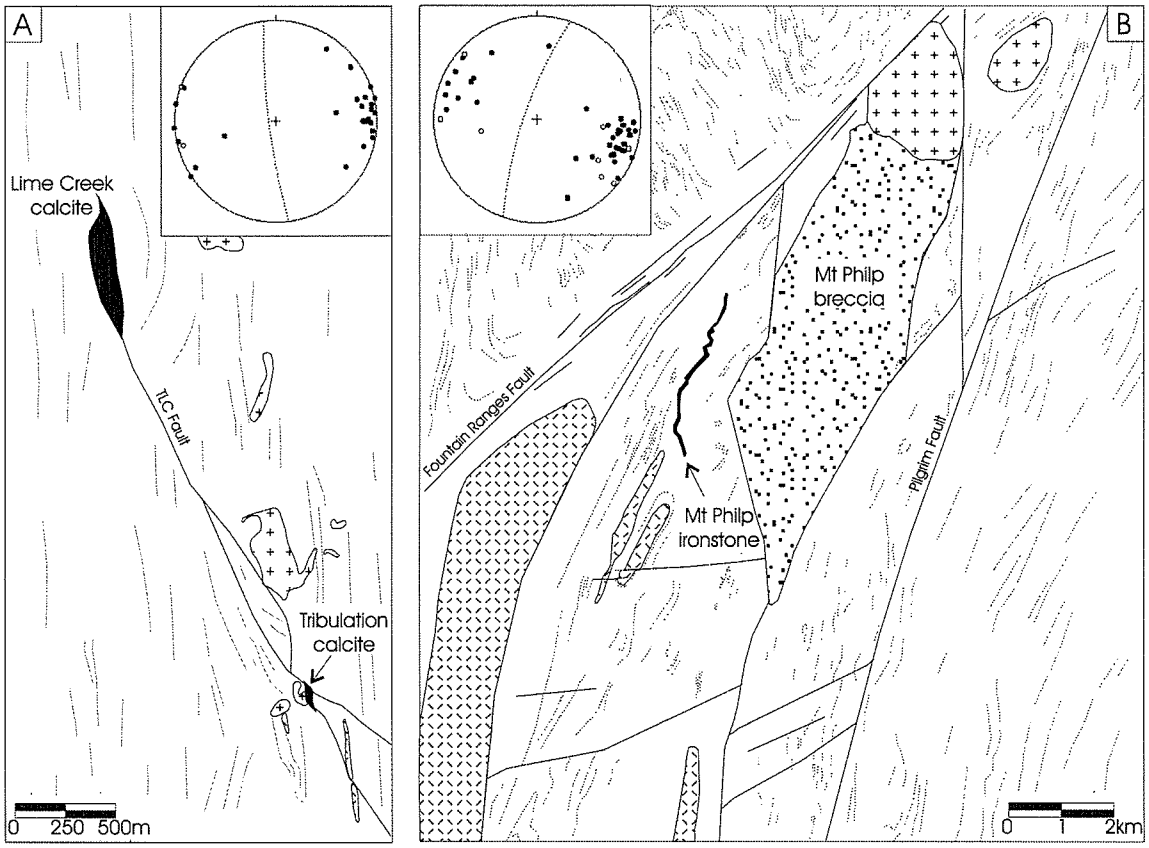

FIGURE 2.4.
Simplified geological maps from the Tribulation and Mt Philp areas. Wongan-aged intrusives (cross hatched) are elongate parallel to the regional structural grain in undifferentiated Cover Sequence 2 wallrocks. Post-peak metamorphic pegmatites (crosses) and breccias (stippled) cut the main structural grain. Stereonets illustrate a consistent N to NNE trend and steep dip to bedding measurements (poles to bedding: filled circles) on fold limbs, and composite S_2/S_3 axial planar fabrics (poles to foliation: open circles). Great circles are fixed to the Beta axis to bedding measurements, and the average of measured axial traces on horizontal surfaces, and as such approximate the orientation of axial planes. Structural measurements are from throughout the map area in Fig. 2.4a, and from between the Fountain Ranges and Pilgrim faults in Fig. 2.4b.

criteria, and is defined for this area only. Correlation with other areas is addressed in the discussion.

D_1 and D_2: Pre- to syn-peak metamorphism structures

The earliest recognized structures in the Cloncurry Region are represented by some of the contacts separating Corella Formation rocks from Soldiers Cap Group rocks (Fig. 2.5). Locally, these contacts are marked by late faults, such as portions of the Cloncurry Fault. More commonly, such as along the western margin of the Pumpkin Gully Syncline, the contact is conformable with, or lies at shallow angles to bedding in both Soldiers Cap Group rocks and Corella Formation rocks, and is folded about subsequent folds (Fig. 2.5). While the contact is itself everywhere topographically recessive, an increase in the intensity of a bedding subparallel schistosity is noted as the contact is approached. This schistosity is interpreted as being related to one or more D_1 shear zones, which, except where offset by late faults, marks the main Corella – Soldiers Cap contact (e.g. Laing, 1998).

In the Cloncurry Region, the D_1 shear contacts between Corella Formation and Soldiers Cap Group rocks are folded about consistently developed tight to isoclinal macroscopic D_2 folds with wavelengths up to 5km, and inferred amplitude of several kilometres. Mesoscopic folds of like morphology and similar local orientation are common within rocks of both Cover Sequences 2 and 3 in the region, although on a regional scale, the orientation of these folds varies considerably. Common doubly plunging folds, and a range from shallow to moderate fold plunges suggest these folds were either superposed on earlier open folds, or had a significant non-cylindrical component. The folds closely approximate Class 2 (similar) folds (classification of Ramsay, 1967) in all rock types, and display a well-developed axial planar cleavage (S_2) defined by the alignment of mica and quartz grains within fine-grained sediments and metabasites of the Soldier's Cap Group. This cleavage is less well-developed in Mary Kathleen Group marbles, siltstones and calc-silicate rocks, but is locally identified by the macroscopic axial plane parallel alignment of biotite grains. Combined, fold morphology and foliation defined by peak

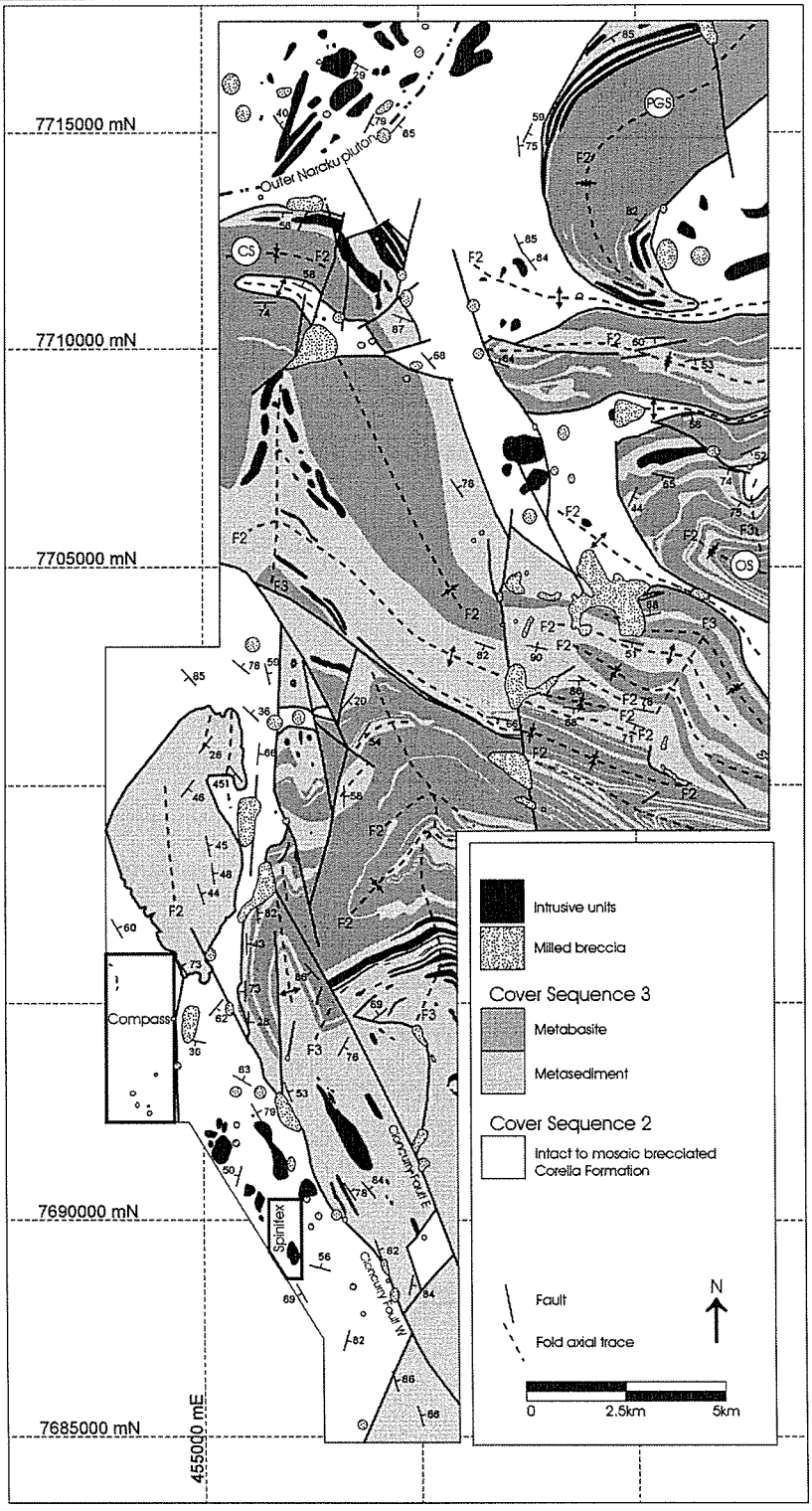

FIGURE 2.5.
Simplified geological map of the Cloncurry Region highlighting the variation in D_2 fold orientations. CS = Cloncurry Syncline, PGS = Pumpkin Gully Syncline, OS = Oonoomurra Syncline. The margin of the Outer Naraku pluton is inferred from geophysical data (see Fig. 2.11). The locations of the Compass and Spinifex areas are indicated.

metamorphic minerals suggests that D_2 folds formed at or close to peak metamorphic conditions.

In the northern portion of the Cloncurry Region, Corella Formation rocks consistently crop out in the cores of D_2 anticlines, indicating that in this area, the Corella Formation underlies the Soldiers Cap Group, the two sequences being separated by D_1 shears as described above. Locally, stratigraphic units in the Soldiers Cap Group do not match across anticlines (Fig. 2.5), a feature interpreted to be a function of the local stratigraphic discordance of the Corella – Soldiers Cap shear contacts.

D_3: Retrograde folding

Early isoclinal folds and associated axial planar cleavages are refolded about open to tight D_3 folds, with most commonly steeply-dipping, northwest to northeast striking axial planes. D_3 folds are only locally developed, with fold amplitudes ranging up to approximately 1 km. These folds commonly form isolated fold crests (Fig. 2.5), and as such typical fold wavelength cannot be defined. Furthermore, D_3 folds commonly die out along the axial trace. Fold morphology is highly variable, with folds in more siliceous and feldspathic horizons approaching Class 1b (parallel) folds, and in more micaceous and/or carbonate rich horizons reflecting Class 2 (similar) and Class 3 folds. Mesoscopic near-axial planar crenulation cleavage (S_3) is locally developed in Soldiers Cap Group rocks, but is typically absent in Corella Formation rocks. Highly variable fold morphology, and the lack of a well-developed axial planar cleavage suggests these folds formed under retrograde metamorphic conditions. Further, metasomatic fluid flow associated with syn-folding brecciation (see **Chapter 4**) has resulted in replacement of peak-metamorphic mineral assemblages.

2.2.5 Superposed fold analysis

Detailed structural mapping was undertaken in two regions of relatively intact marble and calc-silicate rocks within the Cloncurry Region, here termed the Spinifex and Compass areas (Fig. 2.5). Deformation events referred to below are

only defined for the regions in which they are described, with correlation between regions addressed in the discussion.

Spinifex area

Located approximately 22 km southeast of Cloncurry, the Spinifex area comprises a complexly folded sequence of marbles and calc-silicate rocks of the Corella Formation (Figs. 2.6 and 2.7). Corella Breccias surround the region, but within the area calc-silicate rock horizons are only locally veined, and are readily traced on aerial photographs and in the field.

Three episodes of folding are inferred within the Spinifex area. D_2 folds dominate the region, are tight to isoclinal, and except where refolded by D_3 folds, are approximately N-S trending. Fold axes, and L^0_2 intersection lineations are shallowly plunging to the north and south, reflecting the doubly-plunging nature of the folds. It is possible that this is a function of high strain and displacement of D_2 fold axes towards the extension direction (i.e. non-cylindrical folding). Alternatively, a consistent pattern of domes and basins may reflect refolding of inferred D_1, NW-SE trending gentle to open, upright folds, with limbs dipping shallowly to the northeast and southwest. No mesoscale D_1 fold closures were observed, and a mesoscopic axial planar cleavage was not identified, although this may have been destroyed through subsequent deformation.

A third generation of folds is locally developed in the area. These form close folds that refold D_2 axial traces (Fig. 2.6). D_3 folds trend to the NNE, and minor fold axes, lying on the limbs of D_2 folds, plunge steeply to the south (Fig. 2.6). D_3 folds are seen to die out up and down the axial trace.

Compass area

Located 16km SE of Cloncurry, and 6km NW of the Spinifex area, the Compass area contains a complexly folded sequence of marble and calc-silicate rocks similar to those found in the Spinifex area.

At least two fold generations are evident within the area. In the northern Compass area, isoclinal F_2 folds are clearly refolded about an open, reclined F_3 fold,

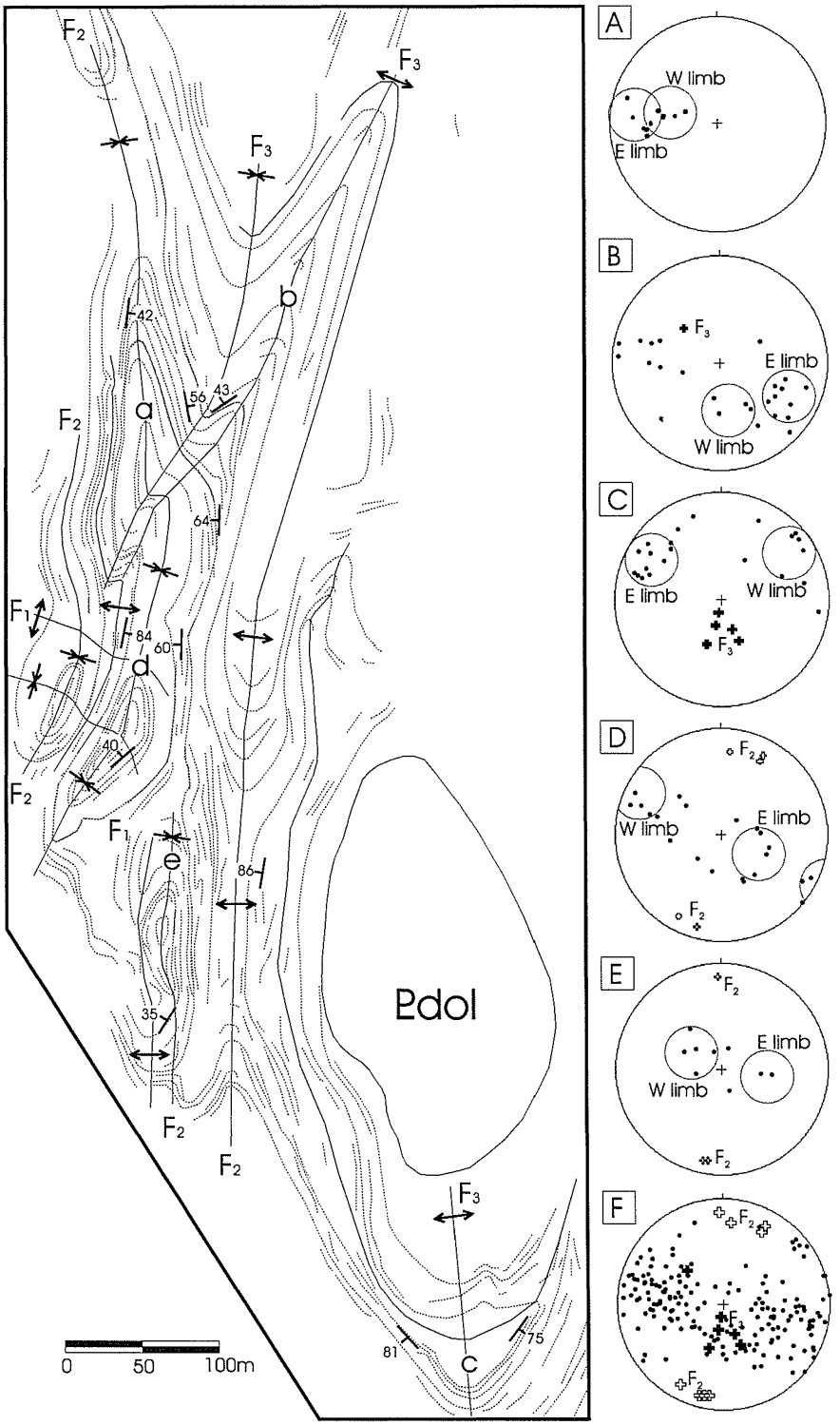

FIGURE 2.6.
Structural map and equal area stereonets illustrating fold geometry in the Spinifex area. (a) Bedding measurements (dots) from both limbs of D2 folds indicate their isoclinal nature. (b) and (c) Bedding measurements and fold axes (filled crosses) from D3 fold limbs and hinge illustrate the open nature of these folds. (d) and (e) Bedding measurements and fold axes (open crosses) from the hinge zones of D2 folds illustrate the doubly plunging nature of D2 folds, as the inferred result of refolding D1 folds. (f) all data.

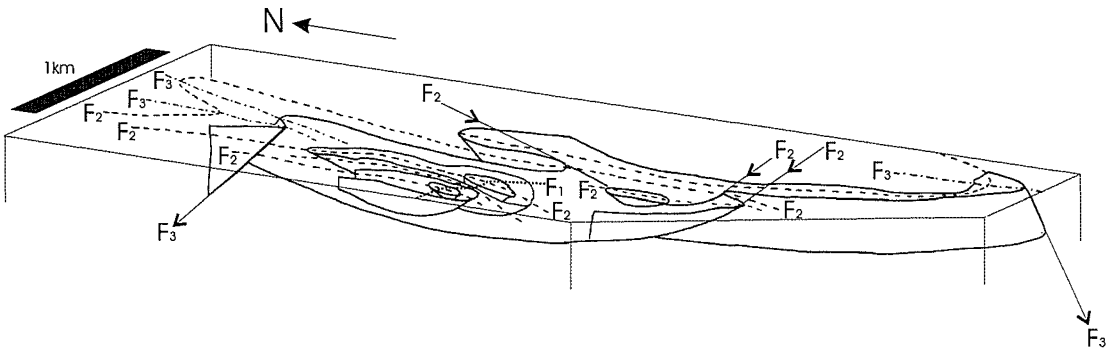

FIGURE 2.7.
Block diagram constructed by 3D projection of structural data using an orthographic net (e.g. McIntyre and Weiss, 1956), illustrating the effect of superposed folding in the Spinifex area.

the axial plane of which dips moderately to the ESE (Figs. 2.8 and 2.9). F_3 fold axes plunge moderately to the east, and poles to bedding are evenly distributed along the great circle to late fold axes. In the central Compass area, while overprinting relationships are unclear, the distribution of bedding measurements is similar to the northern Compass area, but with D_3 fold axes plunging moderately to the SE. In the southern Compass area, overprinting relationships are also unclear as the axial traces of early folds are not consistently bent about later generation folds. This is most consistent with the superposition of two generations of folds with near orthogonal axial planes. Variations in structural trends from north to south are inferred to be a function of reorientation of D_2 structures prior to D_3, and/or variable D_3 shortening directions.

2.2.6 Late fault architecture

Numerous late faults are evident in the Cloncurry Region. These have a dominantly NNW to NNE trend and steep dip, although fault segments are present in all orientations (Fig. 2.5). The faults are most easily identified within Soldiers Cap Group rocks, where they cut and offset stratigraphic units that are readily identified on airphotos and/or geophysical images. Faults are more difficult to recognize within the Corella Formation, as major stratigraphic units are not as distinct as in the Soldiers Cap Group, and stratigraphy is obscured by extensive brecciation. Furthermore, where discrete faults noted in the Soldiers Cap Group cross into Corella Formation rocks, fault zones tend to dissipate into broad breccia zones that become difficult to distinguish from other styles of brecciation (see **Chapters 4** and **5**).

Late faults in the Cloncurry Region cut early shear contacts between the Soldiers Cap and Corella formations, as well as variably oriented fold axial traces. Late faults show consistent apparent lateral offset: sinistral for north- to east-trending faults, and dextral for north- to west-trending faults.

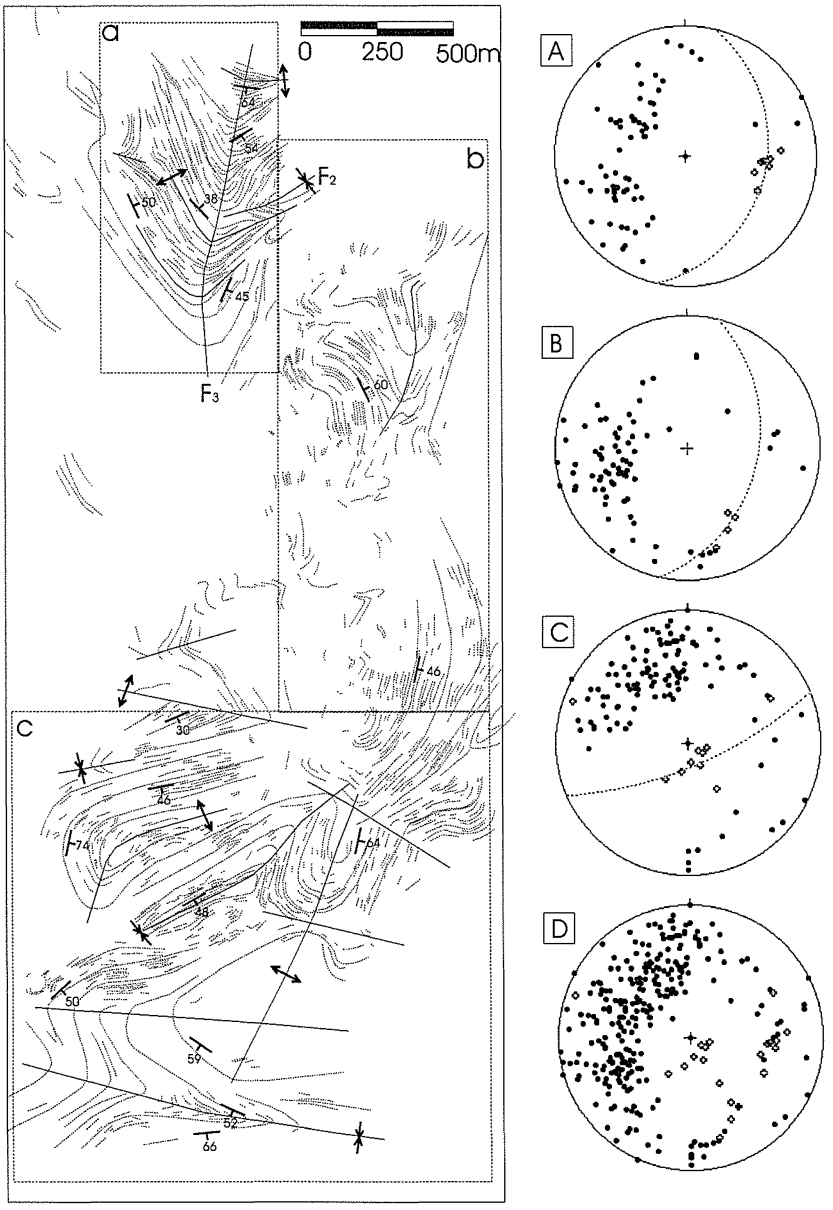

FIGURE 2.8.
Structural map and equal area stereonets illustrating fold geometries in the Compass area. Great circles in each stereonet approximate F_3 axial planes, and are constrained by Beta axes calculated from poles to bedding, and from average orientations of F_3 axial traces on horizontal surfaces. (a) Northern Compass area. Bedding measurements (dots), east-plunging F_3 fold axes (open crosses) and a NNE-trending axial trace indicate an ESE-dipping axial plane for F_3 folds. (b) Central Compass area. Structural data illustrates a similar overall geometry to the northern Compass area, although F3 fold axes plunge to the SSE, likely indicating different bedding orientation (relative to the northern Compass area) at the onset of F_3 folding. (c) Southern Compass area. Fold patterns and near vertical fold axes suggest superposition of two fold episodes with near-orthogonal sub-horizontal shortening directions. (d) All data. Broad variation in F_3 fold axes and axial planes suggest variable orientation of F_2 folds at onset of late folding, and/or heterogeneous strain during late folding.

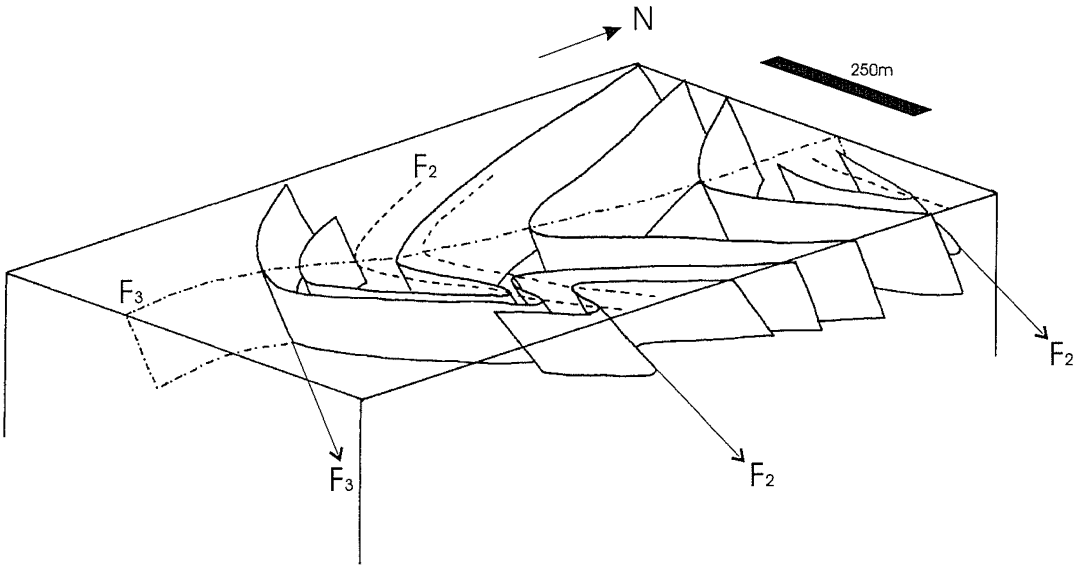

FIGURE 2.9.
Block diagram constructed by 3D projection of structural data using an orthographic net for the northern Compass area illustrating early isoclinal folds refolded by a late fold with east-dipping axial plane.

Cloncurry Fault zone

The Cloncurry Fault forms a major lineament in regional geophysical images, airphotos and geological maps. The fault marks a relatively continuous zone, which stretches nearly 200 km from near Cloncurry in the north, SSE to the southern edge of the Mt Isa Inlier, near the Cannington deposit (Fig. 2.1). Where intersected by the Mt Isa deep seismic transect, the Cloncurry Fault is inferred to dip approximately 45° to the east (MacCready et al., 1998). Along part of its length, the Cloncurry Fault marks the contact between Maronan Supergroup rocks to the East, and Corella Formation rocks to the West. The fault cuts and offsets the Saxby granite (1536 ± 11 Ma; Page and Sun, 1998) indicating a component of post-D_2 movement.

In the southern portion of the Cloncurry Region, the Cloncurry Fault marks the main contact between Soldiers Cap Group and Corella Formation rocks (Fig. 2.5). Here, the fault consists of a series of en échelon NNW trending fault segments that are connected by a complicated array of linking faults and breccia zones. A block of sillimanite-bearing schists of the Soldiers Cap Group is bound by two NNW-trending splays of the Cloncurry Fault, with lower metamorphic grade biotite zone Corella Formation calc-silicate rocks to the west, and sillimanite-free pelitic schists to the east (Rubenach, pers. comm., 2001).

Along some of its length in this region, the Cloncurry Fault is subparallel to stratigraphic layering in both hangingwall and footwall rocks. Elsewhere, the fault cuts early shear contacts which separate Corella Formation and Soldiers Cap Group rocks, leaving some unbrecciated Corella Formation stratigraphy cropping out to the east of the main trace of the Cloncurry Fault (Fig. 2.5).

2.2.7 Cloncurry 3D architecture

Figure 2.10 is a simplified block diagram illustrating the three-dimensional architecture of major lithological and structural contacts east of the Cloncurry Fault in the northern Cloncurry District. The diagram was constructed by orthographic projection of structural data, and with the exception of the dip of the outer Naraku pluton (see below), was constructed independent of any geophysical interpretation.

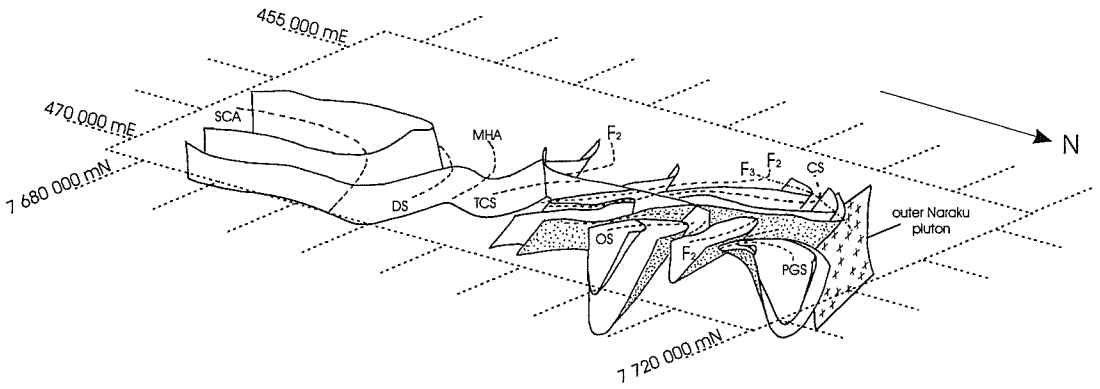

FIGURE 2.10.
Block diagram from the northern Cloncurry District, constructed by orthographic projection of structural data from this study and from Lewthwaite (2000). Grid and top of each surface are at ground level. Stippled surfaces indicate the Corella Formation side of Corella Formation – Soldiers Cap Group contacts. The surface expression of the margin of the outer Naraku pluton is constrained by field observations and aeromagnetic interpretation. The outward dip to the pluton is inferred from wavelet-processed aeromagnetic data (Figure 2.11). SCA = Snake Creek Anticline, DS = Davis Syncline, MHA = Mountain Home Anticline, TCS = Toole Creek Syncline, OS = Oonoomurra Syncline, CS = Cloncurry Syncline, PGS = Pumpkin Gully Syncline.

In Figure 2.11, form surfaces are interpreted from upward projected wavelet-processed aeromagnetic data. Combined, Figures 2.10 and 2.11 provide several insights into the subsurface geometry of the northern Cloncurry District.

Cloncurry Fault zone

Wavelet processed aeromagnetic data confirms the easterly dip to the Cloncurry Fault zone (surface 1 in Fig. 2.11) as interpreted by MacCready et al. (1998). However, the fault is only evident at z-values under approximately 4610m. Along much of its length, the Cloncurry Fault juxtaposes the Soldiers Cap Group against the Corella Formation, sequences that exhibit marked differences in magnetic character in conventional aeromagnetic data. Thus, if the Cloncurry Fault were a deep-rooted structure, one would expect the fault to project to greater z-values in the wavelet processed data. Given that it does not, it seems likely that the Cloncurry Fault is either a) only a near surface structure, b) has a listric geometry, or c) merges with or is cut by a flat lying structure at depth to the east.

Central and Outer Naraku Plutons

A series of worms, easily extrapolated to z-values of 13870m, outline a central pluton within the Naraku Batholith (surface 2 in Fig. 2.11). The geometry of this surface indicates that this pluton dips underneath itself, suggesting that the current exposure cuts through either the lower or middle portion of an inferred central Naraku pluton. Geochronological data indicates that this central Naraku pluton is itself composite, with components emplaced at 1746 ± 8, and 1505 ± 8 Ma (Page and Sun, 1998).

Also evident in the wavelet processed aeromagnetic data is a well-defined surface forming a rim around the eastern and southern margins of the central Naraku pluton (surface 3 in Fig. 2.11). The area between the central pluton and this outer surface is characterized by intermittent outcrops of intensely brecciated and metasomatised Corella Formation and non-foliated granitoids and mafic intrusives (Fig. 2.5), as well as a highly irregular structural grain (Fig. 2.2). The outer surface dips away from the central pluton, rendering it unlikely that this surface

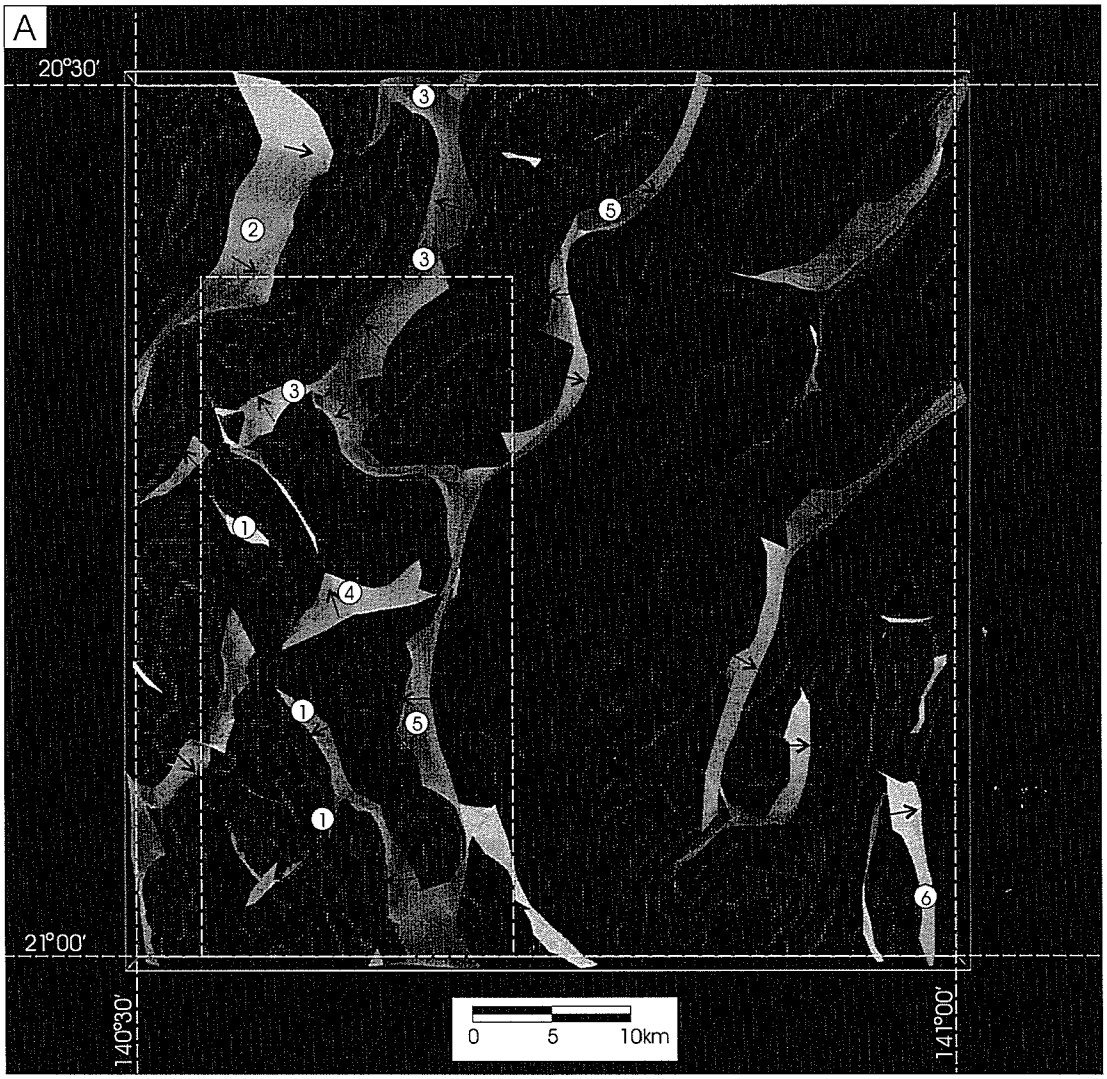

FIGURE 2.11.
(a) gOcad block diagram of upwards projected wavelet processed aeromagnetic data, covering the Cloncurry 1:100000 map sheet. In constructing the figure, curves were fitted to wavelet processed TMI data within eight sections of constant z-value between 2 890 to 8 660m. Curves were not extrapolated between gaps in the wavelet processed data. Form surfaces in the figure were constructed by connecting curves at different z-values. In order to relate these surfaces to exposed geology, wavelet processed data has been plotted as points at low to moderate z-values (200 to 8 660m, 25 sections). The surfaces themselves were not extrapolated to low z-values, as extrapolation between curves becomes increasingly subjective at smaller z-values, as a function of the increasing level of noise in the data. Form surfaces are interpreted as: 1) the Cloncurry fault, 2) an inner Naraku pluton edge, 3) an outer Naraku pluton edge, 4) an unidentified structure (fault?), 5) the Cloncurry Worm and 6) the Levuka shear zone. Arrows indicate approximate dip directions of the surfaces. Because of the upwards projection, structures dip the opposite direction from that indicated in the figure. Dashed rectangle indicates the outline of Figs. 2.10 and 2.13d. Continued on following page.

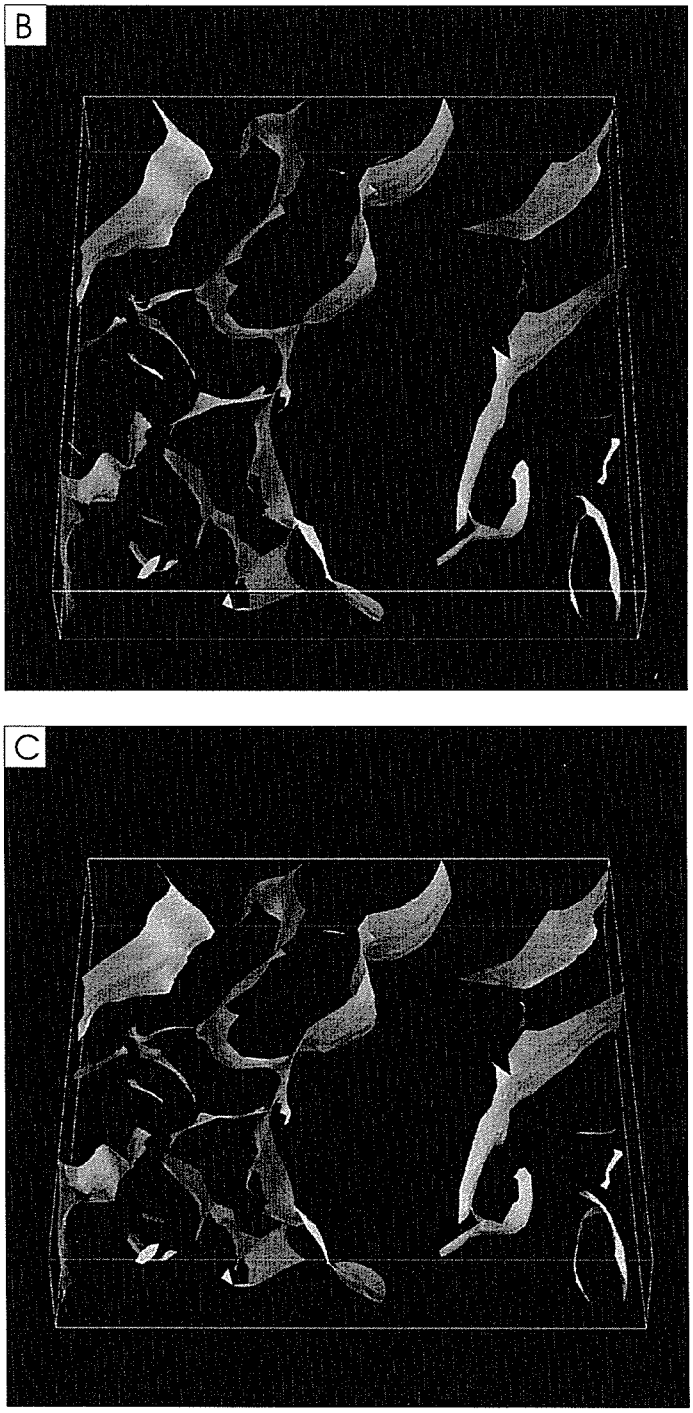

FIGURE 2.11.
(b and c) Perspective view of block diagram in Fig. 2.11a, seen from above and from the south.

represents the margin of a contact metamorphic or metasomatic aureole around the central Naraku pluton. While other interpretations are possible, it seems most likely that this outer surface corresponds to the edge of a younger, outer pluton of the Naraku Batholith. Given the outward dip of this surface, and the mixed metasedimentary and plutonic rocks inside the surface, the current level of exposure appears to be cutting through the roof zone of the inferred outer Naraku pluton.

Toole-Creek – Pumpkin Gully subsurface geometry

The irregular fold trends developed in the northern Cloncurry Region (Figs. 2.2 and 2.5) are difficult to reconcile with the D_1-D_2-D_3 classification scheme of O'Dea et al. (1997). It is noted here that the margins of the Pumpkin Gully and Cloncurry Synclines closely parallel the surface expression of the inferred outer Naraku pluton. Figure 2.11 indicates that this pluton dips outwards to the SE, under the Pumpkin Gully and Cloncurry Synclines, suggesting the parallelism may extend to depth (Fig. 2.10). Potential causes for this parallelism are addressed in the discussion.

Also of note in the northern Cloncurry Region is a broadly E-W striking south-dipping surface (surface 4 in Fig. 2.11). While this surface has a similar strike to overlying fold patterns, it does not correspond well with specific surficial features. One possibility is that this surface represents a deep structure that has affected the geometry of subsequent fold patterns in overlying rocks. For instance, the surface may reflect a south-dipping fault, possibly developed within a Wongan aged décollement zone as described by Holcombe et al. (1991) in the Mary Kathleen Fold Belt, or developed during D_1.

Cloncurry Worm

One of the most striking features in the wavelet processed magnetics data is a roughly N-S trending feature that transects the whole of the exposed Eastern Succession (surface 5 in Fig. 2.11). The feature, here termed the Cloncurry Worm, is visible to z-values up to 25 990m, and is best-imaged at large z-values. At moderate to small z-values, the Cloncurry Worm appears to merge with other

smaller-scale features. In the northern Cloncurry District, there is a marked change in magnetic intensity across the Cloncurry Worm, a feature which might be explained by the surface in places being coincident with a late fault across which there is a marked difference in thickness of flat-lying Paleozoic cover. However, the Cloncurry Worm continues to the south where it cuts Proterozoic exposures to the east and west, and is coincident with the Cloncurry overthrust (Fig. 2.1), a D_1 mylonitic shear zone separating Cover Sequences 2 and 3 (Rubenach, M.J., Blenkinsop, T.G., and Oliver, N.H.S., pers. comm., 2002). The nature of the Cloncurry Worm and its influence on the regional geometry of the Eastern Succession is the subject of ongoing research by other workers.

2.3 DISCUSSION

2.3.1 D_1: Thrusting and folding

Except where offset by late faults, the nature of the Corella – Soldiers Cap contact is interpreted as one or more D_1 shear zones. This is supported by the topographically recessive nature of the contact, the local discordance of the contact with adjacent stratigraphy, and the development of a locally intense shear fabric as the contact is approached. However, the nature of this structure or structures is debatable, and either extensional shears or thrusts can explain the occurrence of younger rocks (Soldiers Cap) faulted over older rocks (Corella). If thrusting is appealed to, then either a) thrusts reactivated earlier extensional structures, or b) thrusting emplaced younger allochthonous Cover Sequence 3 rocks onto the Mount Isa Block (see also O'Dea et al., 1997; Laing, 1998; Betts et al., 2000).

Dome and basin patterns in the Spinifex area may reflect refolding of gentle to open, SE-NW trending folds D_1 folds. However, it is unclear whether these folds were related to D_1 thrusting, and may represent a distinct deformation episode. The folds may be synchronous with early ESE striking cleavages and folds recognized in the Snake Creek area (G_1 of Lewthwaite, 2000), and attributed to an early episode of N-S sub-horizontal shortening.

2.3.2 D_2: E-W shortening and isoclinal folding

Based on fold morphology, and a broad correspondence with peak-metamorphism, tight to isoclinal folds in the Mary Kathleen Fold Belt, the Budenberri region and the Cloncurry region, including the Spinifex and Compass areas, may be broadly synchronous with the D_2 event of O'Dea et al. (1997). However, as warned by previous workers (e.g. Holcombe, 1992; Betts et al., 2000), such a correlation is by nature tenuous in complex orogenic belts. Within the Spinifex area and in the Mary Kathleen Fold Belt, these folds have a uniform orientation that likely reflects folding in response to a period of E-W shortening. However, within the Compass area and broader Cloncurry Region as well as in the Budenberri area, these folds exhibit a variety of orientations. The possibility exists that some of these folds formed during earlier deformation events. Alternatively, local variations in the stress field during folding would be expected to have resulted from stress reorientation around preexisting heterogeneities, including early intrusive bodies (e.g. Oliver et al., 1990), or as a result of reactivation of preexisting faults (Fig. 2.12). Thus, variations in fold orientation may simply reflect variations in local stress fields as opposed to changes in the regional stress field, and by default multiple deformation events.

In the northern Cloncurry District, Lewthwaite (2000) appealed to N-S directed compression and dextral shearing which tightened and rotated D_2 folds into an E-W orientation. However, evidence for syn- or post-D_2 N-S directed shortening is not widely recognized elsewhere in the Eastern Succession, and as such appears to reflect a local effect as opposed to a district-scale tectonic event. In the northern Cloncurry Region, a SSE-dipping surface is evident in wavelet processed aeromagnetic data (Fig. 2.10). While this surface does not correlate well with any single surficial feature, it has a similar orientation to overlying folds. The surface may represent a south-dipping fault developed in the Corella Formation during Wongan extension or during D_1. Either during or subsequent to D_2, dextral shear across this surface may have resulted in a deflection of fold axes in overlying rocks towards E-W. Thus, while other interpretations are possible, anomalous E-W oriented D_2 folds in the Cloncurry Region, and possibly in the Budenberri area, may

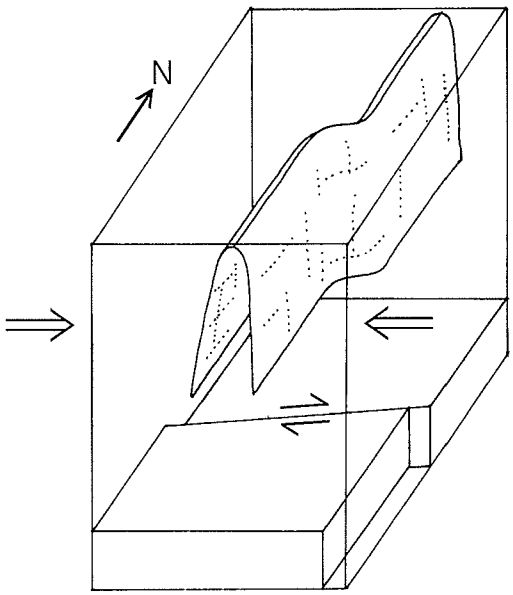

FIGURE 2.12.
Schematic diagram illustrating how the strike-slip reactivation of buried rift-faults may influence the geometry of folds developed in overlying sequences.

be related to reactivation of the early fault architecture at depth. Additionally, folds may have been reoriented subsequent to folding, as described below.

2.3.3 Reorientation of D_2 folds

Several authors have appealed to reorientation of D_2 folds prior to the onset of D_3 (e.g. Mares, 1998; Adshead-Bell, 1998). Associated features include the development of localized crenulation cleavages and rare mesoscopic folds in a variety of orientations. Both gravitational driven orogenic collapse (e.g. Mares, 1998), and the emplacement of the Williams and Naraku batholiths (Betts et al., 2000) have been appealed to in order to explain post-D_2 shallow-dipping cleavages and reorientation of early folds.

Determining the relative importance of strain partitioning and forceful emplacement of plutons is plagued with difficulties (e.g. Paterson and Tobisch, 1988; Molyneaux and Hutton, 2000), particularly where the absolute timing of deformation is poorly constrained. Regardless, the near parallelism of some structural grains with pluton margins (Fig. 2.2) suggests that intrusions played a significant role in governing regional structural trends in the Eastern Succession. However, with the exception of a few studies (e.g. Glikson, 1972; Oliver et al., 1990; Betts et al., 2000), this role has largely been ignored in the Eastern Succession. Notably however for the Cloncurry District, Glikson (1972) proposed that extensive brecciation in the Corella Formation was the result of rotation and cross-folding of early folds, in response to emplacement of the Naraku Batholith.

In the northern Cloncurry District the margins of the Pumpkin Gully and Cloncurry Synclines are nearly parallel to the margin of the outer Naraku pluton (Figs. 2.5 and 2.10). This is interpreted as a combined effect of forceful displacement of wallrocks during pluton emplacement, and subsequent strain partitioning during ongoing deformation. One variation on such a scenario is illustrated in Figure 2.13. Similarly, NW-trending structures in the northern Tommy Creek block and the northern extent of the D_2 Duck Creek Anticline axial trace are broadly parallel to the margin of the Naraku Batholith, and may reflect similar strain reorientation and/or active displacement during pluton emplacement.

Indeed, anastamosing of structural grains around intrusives is common throughout the Eastern Succession (Fig. 2.2), and should not be ignored in structural interpretations. Notably however, some of the later intrusions cross-cut all structural patterns without deflection (Fig. 2.2), which may suggest a change in pluton emplacement mechanism with location and/or time, from (partially) forceful, to stoping dominated (e.g. Paterson and Fowler, 1993).

2.3.4 D_3: E-W shortening, heterogeneous folding, reverse and wrench faulting

Retrograde folds described in this study can be broadly correlated with the widely recognized D_3, E-W directed shortening event across the Eastern Succession. This event was interpreted by O'Dea et al. (1997) as marking a transition to thick-skinned deformation which produced upright folds, broad flexures in the basement-cover interface, and east-dipping basement cutting reverse faults (MacCready et al., 1998). The presence of voluminous pre- and syn-D_3 intrusions may have locally partitioned strain during this event, resulting in the sporadic development, and variable orientation of D_3 folds, particularly in the Cloncurry District, where such intrusions are most abundant. The variability in the orientation of D_3 structures is also noted in studies in the Hampden Synform (Betts et al., 2000), and in the Snake Creek Anticline (G_4 of Lewthwaite, 2000).

The late fault array in the Eastern Succession shows consistent apparent lateral offset on conjugate faults which suggests late fault movement under conditions of predominantly east-west directed shortening (e.g. Laing, 1998). However, in homogenous rocks, east-west directed shortening would result in predominantly ENE and ESE striking faults, as opposed to the dominant NNE to NNW strike and moderate to steep dip of late faults in the Eastern Succession. Thus it seems likely that the geometry of late faults reflects reactivation of earlier structures and/or localization of late faults in regions of crustal weakness developed as the result of earlier deformation. That is, the average north-trend of late faults is a function of the earlier geometry of the terrane, as opposed to representing a fault array optimally oriented with respect to the regional stress axes. Alternatively,

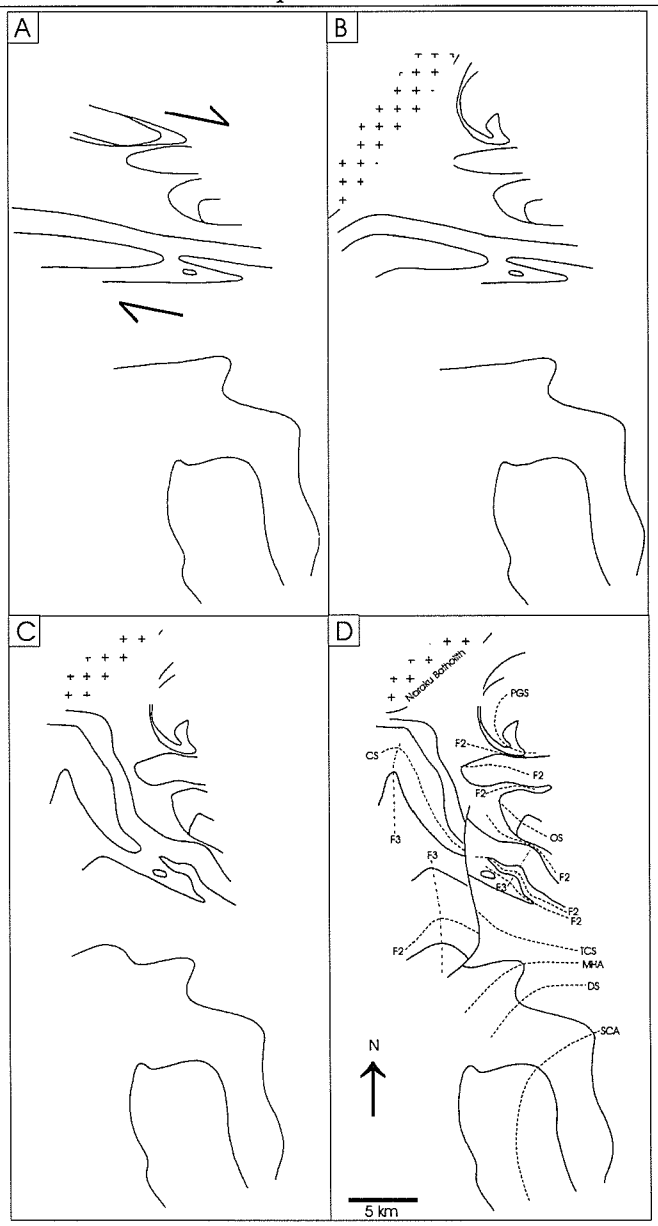

FIGURE 2.13.
Simplified model for the development of anomalous fold patterns in the northern Cloncurry District east of the Cloncurry fault (same area as shown in Fig. 2.10). (a) D_2 folds exhibit a shift from N-S to E-W trends, as the inferred response to dextral shear across rift-related faults at depth, either during or subsequent to D_2 folding, and possibly also reflecting strain partitioning around Wongan-aged phases of the Naraku batholith. (b) Emplacement of younger phases of the Naraku batholith forcefully displaces stratigraphy in the Pumpkin Gully and Cloncurry synclines. (c) D_3 E-W shortening produces local folding in previously E-W trending stratigraphy. (d) Late D_3 faulting results in the present geometry. Note that the relative timing of pluton emplacement and D_3 are poorly constrained, and consequently the effects of b) and c) may be reversed without significant effect on the resultant geometry. SCA = Snake Creek Anticline, DS = Davis Syncline, MHA = Mountain Home Anticline, TCS = Toole Creek Syncline, OS = Oonoomurra Syncline, CS = Cloncurry Syncline, PGS = Pumpkin Gully Syncline.

originally ENE and ESE striking faults may have been rotated towards NNE and NNW strikes during progressive deformation.

Observations along the Cloncurry Fault require a protracted deformation history. Portions of the fault appear to represent an early-tectonic contact between the Soldiers Cap Group and the Corella Formation that has been reactivated, and overprinted by several slip events. A higher-grade block of Soldiers Cap Group rocks between splays of the fault may indicate post-metamorphic reverse movement on the western fault splay, followed by later normal or wrench displacement across the eastern fault splay.

2.4 CONCLUSIONS

The superposition of multiple brittle and ductile deformation episodes has imparted a complex geometry to the Eastern Succession. This geometry reflects one or more sheets of Cover Sequence 3 rocks that have been emplaced and possibly thrust over Cover Sequence 2 rocks during D_1. Lewthwaite argued for D_1 NNE-SSW directed shortening, which may also be recorded in the Spinifex area. The relation between this deformation and early shearing is unconstrained. Early shear contacts and folds were refolded by a sequence of tight to isoclinal, typically N-S trending D_2 folds. Some variation in D_2 fold geometry may have resulted from strain reorientation around early intrusive bodies, and accommodation of strain at depth by reactivation of rift-related faults. In the Cloncurry District, D_2 folds may have been further rotated in response to intrusion of voluminous phases of the Williams and Naraku batholiths. The variable orientation of structures at the onset of D_3 compression, as well as variable local D_3 shortening directions allowed for local refolding, as opposed to simple reactivation and tightening of earlier folds. This overall geometry is further complicated by a series of brittle faults, active during D_3, but largely emplaced during earlier deformation, or simply reactivating earlier structures.

While the nature of early structural features remains poorly constrained, most structural features described in this study can be explained in the context of a protracted history of E-W directed shortening. Regional variations in structural

trends can be explained in terms of strain reorientation and forceful emplacement of plutons, and do not require multiple shifts in compression direction. Thus, observations from this study are in broad agreement with the description of the Eastern Succession as a west-vergent fold and thrust belt (O'Dea et al. 1997).

VOLUME GAIN FOLDING AND EFFECTIVE LAYER THINNING AS MODIFICATIONS ON MODELS OF TANGENTIAL LONGITUDINAL STRAIN

VOLUME GAIN FOLDING AND EFFECTIVE LAYER THINNING AS MODIFICATIONS ON MODELS OF TANGENTIAL LONGITUDINAL STRAIN

3.1 INTRODUCTION

Folds developed in layered rocks exhibit a wide range of shapes, sizes and forms that have intrigued geologists for many years. Early approaches to classify folds proposed different characteristic geometries as end-member fold classes, giving rise to terms such as parallel and similar folds (Van Hise, 1896). Dip isogon analysis (Elliot, 1965) has provided a useful graphical means of characterizing folds, and led Ramsay (1967) to develop his isogon-based geometric classification. Along with the development of increasingly sophisticated geometric classification schemes, researchers have also addressed the link between deformation mechanisms and fold geometry. Various fold mechanisms have been proposed, the most enduring of which include tangential longitudinal strain, flexural flow, flexural slip, heterogeneous simple shear and homogenous strain or pure shear acting on pre-existing folds.

Tangential longitudinal strain is arguably the best-suited model for studying the state of stress and strain within buckled competent layers. This model predicts inner arc shortening and outer arc extension with maximum strain occurring at fold hinges. Extensional fractures associated with these folds are predicted to form in the outer arc of competent layers, and only at fold hinges. However, deviations from the predicted geometry and location of fold-related extensional fractures are common (e.g. Cosgrove and Ameen, 2000; Lemiszki et al., 1994; Ismat and Mitra, 2001; Engelder and Peacock, 2001). Where fractures form during folding, these will have a pronounced effect on the rheologic properties of the layer(s) in which they form, and will affect the geometry of subsequent folding and fracturing, as well as influencing the permeability of layered sequences. As a consequence, established models of buckle folding of intact sheets need not strictly apply following initial fracture. In this contribution, volume gain folding and effective layer thinning are proposed as variations on models of tangential longitudinal strain that may result from the formation of outer arc extensional fractures during folding. These

variations can be used to explain the occurrence of fold related extensional fractures that transect competent layers, rather than being arrested at a neutral surface within the layer as predicted by classical models for tangential longitudinal strain. The analysis is based on theoretical application and modifications of existing theories, stimulated by field observations in the study area.

3.2 REVIEW OF FOLDING MECHANISMS

Passive or similar folds are the product of ductile deformation by means of heterogeneous simple shear with or without a component of homogenous strain (Ramsay, 1967). Pre-existing layers do not play an active role in the deformation process, and only serve as reference markers that record the fold process. These folds develop where viscosity contrast across layers is very small (Fig. 3.1), and as such form under high temperature, high pressure conditions (Biot, 1965; Ramsay, 1967; Parrish et al., 1976).

Folds formed in response to layer parallel contraction in which internal layers of contrasting rheology play an active role in folding are termed buckle folds. Strain distribution within a buckled layer depends on the degree to which strain is accommodated by flexural flow, flexural slip or tangential longitudinal strain.

Flexural flow involves shear parallel to layer surfaces, distributed evenly throughout individual layers. Strain at a given point in a fold is a function of the slope of the layer, and for buckled infinite sheets reaches a maximum on fold limbs while no strain is predicted at fold hinges. Flexural flow has previously been considered a viable method of deformation in buckled competent layers which have a high degree of layer parallel anisotropy (e.g. Ramsay, 1967; Hobbs et al., 1976). However, Hudleston et al. (1996) showed that the degree of anisotropy within most buckled competent layers is insufficient to allow flexural flow to occur (Fig. 3.1). Nonetheless, Hudleston et al. (1996) noted that flexural flow can approximate the overall strain distribution in multilayers of competent and incompetent lithologies. Similarly, flexural slip predicts strain to be largely accommodated by slip at layer boundaries, but does not adequately address the state of strain within competent layers.

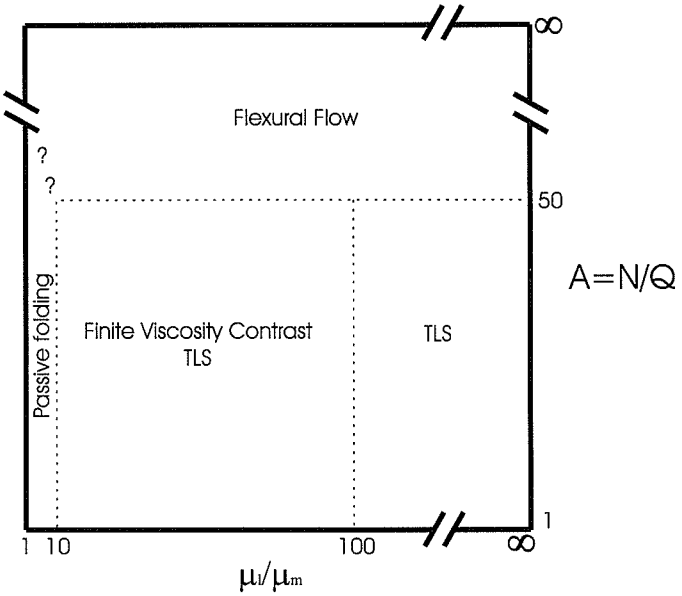

FIGURE 3.1.
Plot of anisotropy (A=N/Q, where Q is the viscosity for shear stress and N the viscosity for normal stress) within a single competent layer vs. the competence contrast between the layer and a homogenous matrix (μ_i/μ_m). The plot defines fields over which models for passive folding, flexural flow, TLS and TLS with the effects of a matrix with finite viscosity are valid. Field boundaries are approximate only, and based on values given by Hudleston et al. (1996), and Dieterich and Carter (1969).

3.2.1 Tangential Longitudinal Strain

The distribution of stress and strain within buckled isotropic competent layers is best described in terms of tangential longitudinal strain (TLS). Tangential longitudinal strain is strictly valid only for isotropic competent layers embedded in a theoretical matrix of zero viscosity, and Young's modulus of zero, where stress can only be propagated along competent layers. Nonetheless, where competence contrasts are high (>100), tangential longitudinal strain provides a good approximation of the distribution of stress and strain within buckled layers (Fig. 3.1).

In previous geometric studies of strain distribution in theoretical TLS folds (e.g. Ramsay, 1967; Bobillo-Ares et al., 2000) a neutral surface has been imposed within buckled layers. Along this theoretical surface there is no finite strain, and by definition the surface maintains a constant length during folding. Strain in the outer arc (outside the neutral surface) is extensional, while strain in the inner arc is contractional (Fig. 3.2). Thinning of the outer arc and thickening of the inner arc are predicted in order to maintain constant area both inside and outside the neutral surface (Fig. 3.2). For single layers where wavelength for a given bulk strain is governed by layer thickness and viscosity contrast, strain accumulation is independent of layer thickness. However, where a given wavelength is imposed on a fold, because of stacking of multilayers of different thickness and competence, greater strains are accumulated in thicker layers. The magnitude of strain is much greater in the inner arc of folds than in the outer arc (Fig. 3.2b). This observation led Ramsay (1967) to suggest that a buckled layer might not be able to accommodate such high inner arc strain. As a result, one of the following may occur: 1) the region of maximum curvature may migrate away from the hinge zone towards the fold limbs; 2) the neutral surface may migrate towards the inner arc (Figs. 3.2c,d); 3) internal deformation may be increasingly accommodated through flexural slip along failure planes developed parallel to layer boundaries, and; 4) conjugate shear failure may occur in the inner arc.

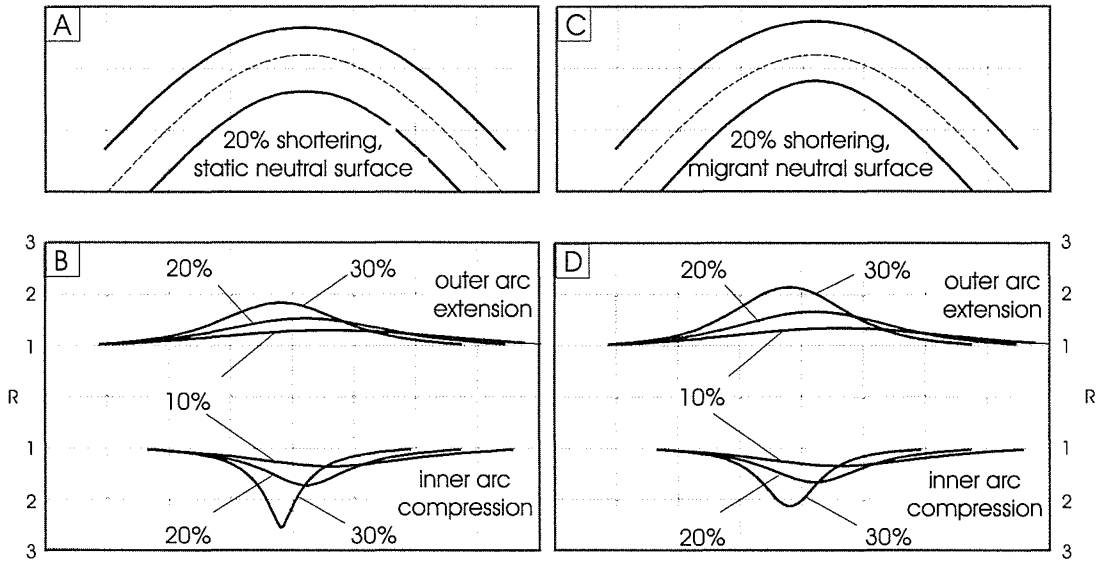

FIGURE 3.2.
(a) Profile section of a theoretical sinusoidal Class 1B fold, shortened 20%, based on the tangential longitudinal strain equations of Bobillo-Ares et al. (2000), with a static neutral surface, fixed such that the inner and outer arcs maintain constant area. The dashed line indicates the finite neutral surface. Note the thinning of the outer arc and thickening of inner arc at the hinge, in order to maintain constant area. (b) Measure of the strain ratio, R, for the fold in Fig. 3.2a at 10, 20 and 30% layer shortening. Strain ratio curves are plotted relative to the left-hand end of each layer. Note that the greatest strains are reached at the fold hinge, and inner arc compressive strains exceed outer arc extensional strains. (c) As in Fig. 3.2a but for folds in which the neutral surface is allowed to migrate in order to equalize the strain ratio in the inner and outer arcs. Note the migration of the neutral surface towards the inner arc, relative to the fold in Fig. 3.2a. (d) Measure of the strain ratio, R, for the fold in Fig. 3.2c at 10, 20 and 30% layer shortening.

With decreasing competence contrast between the layer and matrix, strain distribution increasingly reflects that predicted for homogenous strain (e.g. Dieterich and Carter, 1969). Tensile stresses can be achieved in the fold limbs, and principal stress axes depart from normal and tangential to competent layer boundaries (e.g. Dieterich and Carter, 1969; Engelder and Peacock, 2001). At low competence contrast, tensile stresses do not develop without the influence of fluid overpressuring.

3.3 VARIATIONS ON MODELS FOR TLS

In theoretical models of TLS, the occurrence of both a compressional inner arc and extensional outer arc are functions of a finite neutral surface being imposed on the buckled layer(s). Although these features are well supported by many natural examples, the concepts of a neutral surface, and its occurrence within a buckled layer are in themselves theoretical, and need not apply to all examples of buckle folding. Migration of the neutral surface has been discussed by several authors (e.g. Hills, 1963; Ramsay, 1967; Bobillo-Ares et al., 2000), and has been demonstrated in experimental folds by Gairola (1978). Processes that allow for migration of the neutral surface towards the inner arc of competent layers will also allow extensional fractures to penetrate further into competent layers (Fig. 3.3). Here, 'volume gain folding' and 'effective layer thinning' are proposed as two mechanisms that may aid in neutral surface migration towards the inner arc and account for the formation of fold-related extensional fractures that transect competent layers.

3.3.1 Volume gain folding

Most models of tangential longitudinal strain (e.g. Bobillo-Ares et al., 2000) require that buckled layers maintain constant area in profile section. In nature, dissolution creep is recognized as an important deformation process (e.g. Rutter, 1983) and there is no inherent reason why material removed by dissolution need be precipitated in the same layer, particularly in areas of high fluid flux (e.g. Etheridge et al., 1984). Thus the assumption of constant area need not hold. If material removed from the inner arc is taken out of the layer, deformation within competent

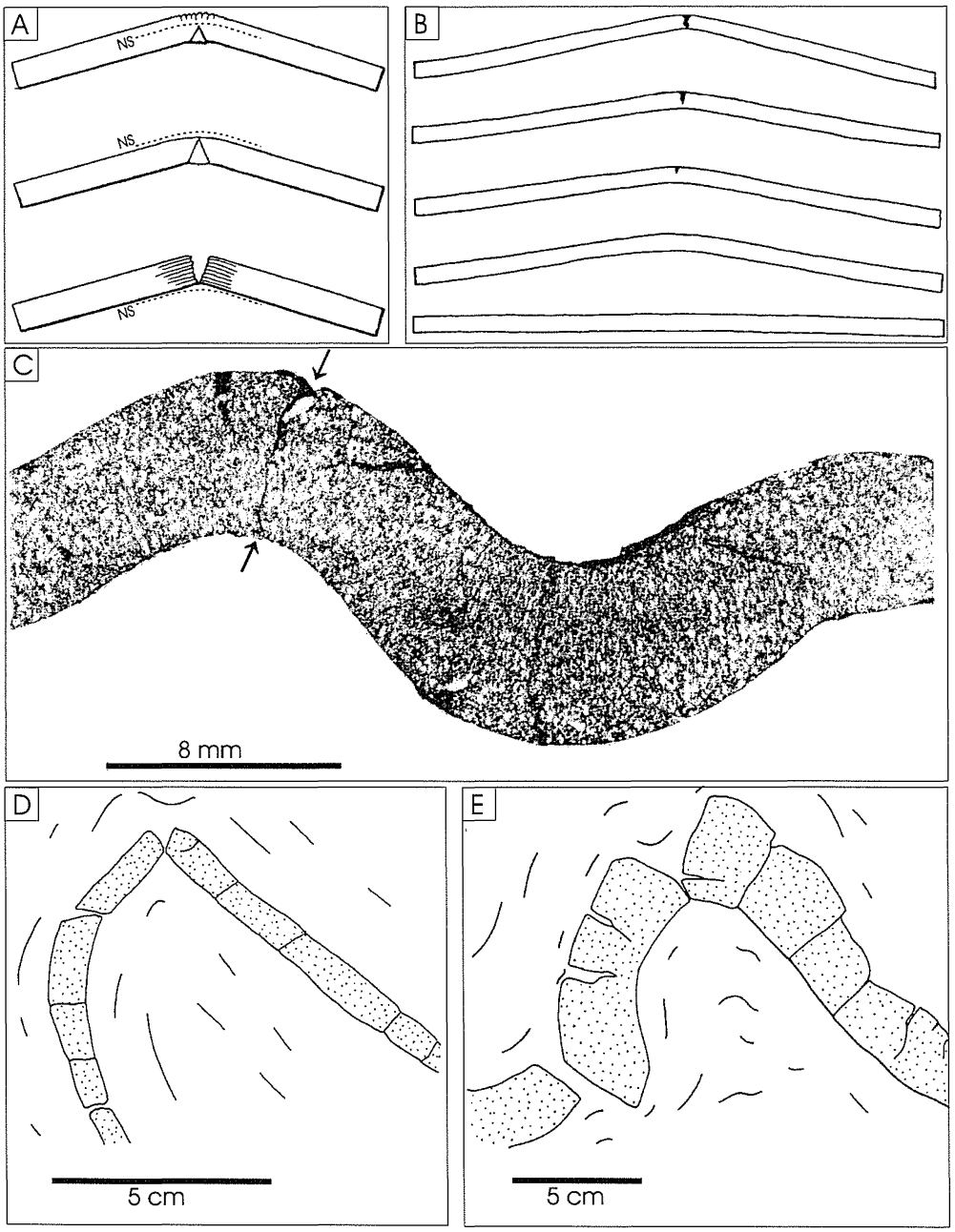

FIGURE 3.3.
(a) Variations in the position of the neutral surface during buckle folding result in areas of hinge zone compression, extension, or both. Modified from Hills (1963). (b) Sketches from photographs of sandstone beams experimentally folded by Handin et al. (1972). Beams permanently shortened between <0.1, and 1.5% (from bottom to top). Note the development of an outer arc extension fracture. As folding progressed, the fold limbs rotated rigidly, and the extensional crack propagated through the layer. Modified from Handin et al. (1972) and Price and Cosgrove (1990). (c) Extensional crack developed in the outer arc of a buckled layer of artificial polycrystalline rock salt embedded in a Plasticine matrix, experimentally folded by Gairola and Kern (1982). The crack has propagated from the outer arc through to the inner arc. (d and e) Sketches from photographs of interlayered marble (unornamented) and siltstone (stippled) in the Corella Formation, Mt Isa Block. Shortening has been accommodated in part by rigid body rotation of calc-silicate rock clasts, separated by extensional cracks. However, in these natural examples, the timing of fracture genesis can only be constrained to pre- or syn-buckling. Scar folding records flow of marble into the inter-clast spaces.

layers can be accommodated to a greater degree (or entirely) by inner arc shortening, with limited or no outer arc extension. This is equivalent to volume-loss folding (Twiss and Moores, 1992, p.242). Conversely, if extensional fractures formed in the outer arc fill with material derived from outside the competent layer, deformation in the competent layer can proceed to a greater degree (or entirely) by outer arc extension (Fig. 3.4a). This will result in migration of the neutral surface towards the inner arc, and is referred to here as volume gain folding. Such a situation may arise where extensional fractures fill with minerals precipitated from externally derived hydrothermal fluids, or where less competent material from adjacent layers is able to ductily flow into extensional fractures, in the form of scar folds (Fig. 3.3e).

3.3.2 Effective layer thinning

In situations where extensional fractures are filled with a material that is less competent than the layer in which they form, that layer will behave as a non-planar sheet. In the vicinity of extensional fractures this may result in the effective inwards migration of the infinitesimal neutral surface (Fig. 3.4b; see also Price and Cosgrove, 1990, p.382). This migration will allow fractures to propagate further into the layer. So long as the fractures are filled with material that is less competent than the layer, then the neutral surface and extensional fractures should be able to propagate completely through the layer. Incompetent material in extensional fractures may be either derived from within the layer or external to it. In the latter case, effective layer thinning may act in tandem with volume gain folding to promote neutral line migration.

Quartz and carbonate minerals are the common fracture-filling minerals, and have very different competencies at a wide range of temperatures (e.g. Parrish et al., 1976). Because grain-size-sensitive flow occurs in carbonates much more readily than in quartz, carbonates will be less competent than quartz under most geologic conditions (Brodie and Rutter, 2000). Consequently, a generalization may be drawn that where fold-related extensional fractures are dominantly filled with carbonates,

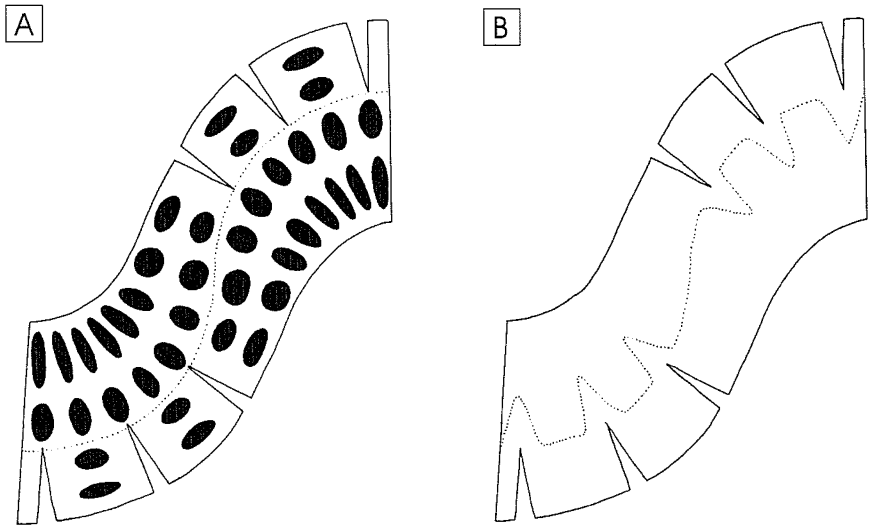

FIGURE 3.4.
(a) Volume gain folding. A component of outer arc extension is accommodated by extensional fractures filled with material derived from outside of the layer, and as such is independent of inner arc shortening. As a consequence of deformation being accommodated to a greater degree by outer arc extension than by inner arc shortening, the infinitesimal neutral surface (dotted line) lies closer to the inner arc. (b) Effective layer thinning. Extensional fractures filled with a low competence material cause the layer to act as a non-planar sheet, and result in the deflection of the infinitesimal neutral surface (dotted line) towards the inner arc in the vicinity of the fractures.

effective layer thinning will be more effective than where extensional fractures are filled with quartz.

3.4 DISCUSSION

Neutral line migration towards the inner arc, by either volume gain folding or effective layer thinning, is essentially the outcome of situations where it is easier for deformation within a competent layer to be accommodated by brittle failure in the outer arc than through inner arc shortening. A number of factors may favor this. For example, at low temperatures, the rate of strain hardening may exceed the rate of dynamic recrystallisation, rendering deformation by dislocation creep increasingly difficult with increased strain. Similarly, if dissolution creep is dominated by the dissolution of one mineral, the abundance of that mineral may limit the amount of total strain accommodation. As inner arc shortening by dislocation creep and/or dissolution creep becomes more difficult, then folding may proceed by increased outer arc extension. If grain-scale processes are unable to accommodate increased outer arc extension, macroscopic brittle failure in the form of extensional fractures may occur. Factors that will promote extensional failure include elevated strain rate, low differential stress, high fluid pressure and the presence of initial cracks or irregularities (e.g. Etheridge et al., 1984; Lemiszski et al., 1994).

Clearly, fractures formed during folding will affect the geometry of subsequent folds and/or fracture propagation. As argued above, this may result in scenarios where fold-related extensional fractures are propagated through competent layers. However other consequences are also possible, for example, fractures may cause the effective layer thickness and layer geometry to change such that new buckle folds of different wavelength begin to form.

3.5 CONCLUSIONS

Volume gain folding and effective layer thinning are proposed as modifications on models of tangential longitudinal strain. These mechanisms, combined with the findings of previous authors, suggest that it is possible to form

extensional fractures during buckle folding that transect competent layers. Extensional fractures will predominate at fold hinges as predicted by models of tangential longitudinal strain, but extensional shear failure can also occur along fold limbs (e.g. Engelder and Peacock, 2001), particularly as limbs are rotated closer to orthogonal to the direction of regional shortening. Extensional failure will occur orthogonal to bedding at fold hinges, and extensional shear can form oblique to bedding on fold limbs (e.g. Dieterich and Carter, 1969; Engelder and Peacock, 2001).

The propagation of fractures completely through buckling competent layers has important implications for the further development of such folds. Where fractures fill with a weak material that has a similar competence to the matrix, the competent layer may cease to act as an intact layer, and will deform instead as a series of isolated competent blocks or clasts within an incompetent matrix. Buckling will no longer be an appropriate model to describe subsequent deformation, which will likely approach homogenous pure shear, although variations in the stress and strain fields would be expected around rigid clasts. Resulting fold patterns may be highly complex, to the point of being unrecognizable as fold structures, or such that fractures cannot be unambiguously related to the fold process (see **Chapter 4**). The development of throughgoing fractures will also affect permeability and fluid flow during folding, and as such has implications for migration and trapping of both hydrocarbons and metalliferous fluids.